

## Title Page

# Functional selectivity in CB<sub>2</sub> cannabinoid receptor signaling and regulation: implications for the therapeutic potential of CB<sub>2</sub> ligands

Brady K. Atwood, James Wager-Miller, Christopher Haskins, Alex Straiker and Ken  
Mackie

Department of Psychological and Brain Sciences, Gill Center for Biomolecular Science,  
Indiana University, Bloomington, Indiana (B.K.A., J.W.-M., C.H., A.S. and K.M.)

## Running Title Page

**Running Title:** Functionally selective CB<sub>2</sub> ligands

**Correspondence:** Ken Mackie, Department of Psychological and Brain Sciences,  
Indiana University, 1101 E. 10th Street, Bloomington, IN 47405, USA (e-mail:  
kmackie@indiana.edu) 812-855-2042 (PH), 812-856-7187 (FAX).

Text Pages: 36

Figures: 6

Tables: 1

References: 53

Words:

    Abstract: 247

    Introduction: 726

    Discussion: 1464

Supplemental Material

Supplemental Figures: 6

Supplemental Tables: 1

**Abbreviations:**

2-AG: 2-arachidonoylglycerol

2-AGE: 2-arachidonoylglyceryl ether (noladin ether)

AEA: anandamide

BSA: bovine serum albumin

CB<sub>1</sub>: cannabinoid receptor subtype 1

CB<sub>2</sub>: cannabinoid receptor subtype 2

ERK: extracellular signal related kinase

FAAH: fatty acid amide hydrolase

GPCR: G protein coupled receptor

HA: hemagglutinin 11

hCB<sub>2</sub>: human CB<sub>2</sub>

HBS: HEPES buffered saline

HEK: human embryonic kidney

MAPK: mitogen activated protein kinase

mCB<sub>2</sub>: mouse CB<sub>2</sub>

MGL: monoacylglycerol lipase

mRFP: modified red fluorescent protein

OEA: oleoylethanolamide

PEA: palmitoylethanolamide

PB: phosphate buffer

PFA: paraformaldehyde

PBS: phosphate buffered saline

PTX: pertussis toxin

rCB<sub>1</sub>: rat CB<sub>1</sub>

rCB<sub>2</sub>: rat CB<sub>2</sub>

TBS: Tris-buffered saline

THC:  $\Delta^9$ -tetrahydrocannabinol

VGCC: voltage gated calcium channel

## Abstract

Receptor internalization increases the flexibility and scope of GPCR signaling. CB<sub>1</sub> and CB<sub>2</sub> cannabinoid receptors undergo internalization following sustained exposure to agonists. However, it is not known if different agonists internalize CB<sub>2</sub> to different extents. Since CB<sub>2</sub> is a promising therapeutic target, understanding its trafficking in response to different agonists is necessary for a complete understanding of its biology. Here we profile a number of cannabinoid receptor ligands and provide evidence for marked functional selectivity of cannabinoid receptor internalization. Classical, aminoalkylindole, bicyclic, cannabiolactone and iminothiazole cannabinoid, and endocannabinoid ligands varied greatly in their effects on CB<sub>1</sub> and CB<sub>2</sub> trafficking. Our most striking finding was that WIN55,212-2 (and other aminoalkylindoles) failed to promote CB<sub>2</sub> receptor internalization, while CP55,940 robustly internalized CB<sub>2</sub> receptors. Furthermore, WIN55,212-2 competitively antagonized CP55,940-induced CB<sub>2</sub> internalization. Despite these differences in internalization, both compounds activated CB<sub>2</sub> receptors as measured by ERK1/2 phosphorylation and recruitment of  $\beta$ -arrestin<sub>2</sub> to the membrane. In contrast, while CP55,940 inhibited voltage-gated calcium channels via CB<sub>2</sub> receptor activation, WIN55,212-2 was ineffective on its own and antagonized the effects of CP55,940. Based on the differences we found between these two ligands we also tested the effects of other cannabinoids on these signaling pathways and found additional evidence for functional selectivity of CB<sub>2</sub> ligands. These novel data highlight that WIN55,212-2 and other cannabinoids show strong functional selectivity at CB<sub>2</sub> receptors and suggest that different classes of CB<sub>2</sub> ligands may

produce diverse physiological effects, emphasizing that each class needs to be separately evaluated for therapeutic efficacy.

## Introduction

Cannabinoid receptors are the targets of both endogenous cannabinoids (endocannabinoids) as well as exogenous cannabinoids such as  $\Delta^9$ -tetrahydrocannabinol (THC) (Howlett et al., 2002). The CB<sub>1</sub> cannabinoid receptor is abundant within the brain, (Mackie, 2005) while the CB<sub>2</sub> cannabinoid receptor is primarily localized in immune cells of both the periphery and the central nervous system. It is possible that it may be expressed in neurons, but the extent and level of expression remain controversial (Atwood and Mackie, 2010). Both CB<sub>1</sub> and CB<sub>2</sub> are GPCRs that couple to the G<sub>i/o</sub> class of G proteins. As such they negatively couple to adenylyl cyclase and both are capable of activating p42/44 MAPK (ERK1/2) (Felder et al., 1995; Howlett et al., 2002).

The CB<sub>2</sub> cannabinoid receptor is an attractive therapeutic target. CB<sub>2</sub> activation is immunomodulatory and neuroprotective (Berdyshev, 2000; Cabral and Griffin-Thomas, 2009; Howlett et al., 2002). CB<sub>2</sub> agonists also suppress both acute and neuropathic pain responses (Anand et al., 2009). Since CB<sub>1</sub> likely mediates most, if not all, of the psychoactive effects of cannabinoids (Huestis et al., 2001; Mackie, 2005; Monory et al., 2007), CB<sub>2</sub> selective agonists are attractive as therapeutics as they would presumably lack this psychoactivity. CB<sub>2</sub> expression also increases under certain conditions and disease states, further adding to its attractiveness as a therapeutic target (Wotherspoon et al., 2005; Yiangou et al., 2006; Zhang et al., 2003).

However, CB<sub>2</sub> agonist-based therapies for many indications will necessitate long-term treatment. Long-term treatment with a GPCR agonist produces a number of physiological adaptations at both the systems and cellular levels. For instance repeated morphine administration produces profound physiological tolerance (von Zastrow et al., 2003). At the cellular level this prolonged exposure results in mu opioid receptor desensitization (Koch et al., 2005), a functional decoupling of the receptor from its G proteins. Extended exposure to opioids also produces mu opioid receptor internalization (Koch et al., 2005). It has been suggested that there is an inverse relationship between mu opioid receptor internalization and desensitization (Finn and Whistler, 2001; Koch and Holtt, 2008; Koch et al., 2005; Whistler et al., 1999). This may also be true for CB<sub>1</sub> cannabinoid receptors. WIN55,212-2 is a cannabinoid receptor agonist that produces substantial CB<sub>1</sub> internalization (Hsieh et al., 1999), but less receptor desensitization than THC, an agonist that produces low receptor internalization (Wu et al., 2008).

Little is known about CB<sub>2</sub> receptor internalization. There is evidence from expression systems that CB<sub>2</sub> undergoes constitutive activation resulting in a basal level of internalization. A CB<sub>2</sub> agonist, CP55,940, enhances internalization whereas SR144528, a CB<sub>2</sub> receptor inverse agonist prevents it, increasing cell surface CB<sub>2</sub> (Bouaboula et al., 1999). A recent study found that HU-308 promotes CB<sub>2</sub> internalization and this internalization can be reversed by AM630. This study also found that AM630 acted as an inverse agonist in regards to internalization (Grimsey et al., 2011). If CB<sub>2</sub> agonists will be used therapeutically, then a greater understanding of the cellular compensations



that occur during lengthy drug treatments will be necessary. Here we characterized a selection of distinct cannabinoid ligands from a number of different structural classes to determine their ability to internalize CB<sub>2</sub> receptors. We hypothesized that potent and efficacious CB<sub>2</sub> agonists would produce greater amounts of internalization than those of lower potency and efficacy. Furthermore, we expected that ligands that were highly selective for CB<sub>2</sub> over CB<sub>1</sub> would produce greater internalization of CB<sub>2</sub> than CB<sub>1</sub>.

Our investigation of CB<sub>2</sub> receptor internalization, led us to explore the functional selectivity of CP55,940 and WIN55,212-2, two of the most frequently used cannabinoid agonists, at CB<sub>2</sub>. Functional selectivity is an important emerging pharmacological concept that describes the ability of different receptor ligands to produce distinct cellular responses due to the activation of differing repertoires of signaling pathways (Urban et al., 2007). There is evidence that some CB<sub>2</sub> agonists display functional selectivity (Shoemaker et al., 2005). In addition to measuring internalization due to CP55,940 and WIN55,212-2, we also measured CB<sub>2</sub>-mediated MAPK activation,  $\beta$ -arrestin<sub>2</sub> membrane recruitment and inhibition of voltage gated calcium channels. These studies found that while CP55,940 was an efficacious agonist for all signaling pathways studied, WIN55,212-2 displayed profound functional selectivity, activating only a few of these signaling pathways. In addition to WIN55,212-2 we found that several other CB<sub>2</sub> agonists exhibited significant functional selectivity in these cellular signaling pathways.

## Materials and Methods

**Reagents.** Drugs and reagents were purchased from Tocris Cookson (Ellisville, MO), Cayman Chemical (Ann Arbor, MI), Invitrogen (Carlsbad, CA), Thermo Fisher Scientific (Waltham, MA), LI-COR Biosciences (Lincoln, NE), Gibco Life Technologies (Rockville, MD), Clontech (Mountain View, CA) or Sigma-Aldrich (St Louis, MO). JWH018 was synthesized as described in (Huffman et al., 1994). CP55,940, Rimonabant (SR141716), SR144528 and THC were obtained from the National Institute of Drug Abuse Drug Supply Service. A-836339 was generously provided by Abbott Laboratories (Abbott Park, IL), AM1710 was from Andrea Hohmann (Indiana University) and HU210 from Dr. Raphael Mechoulam (Hebrew University). CP47,497-C8 was synthesized as described in (Atwood et al., 2011). THCV was obtained from Aron Lichtman (Virginia Commonwealth University).

Mouse anti-HA11 antibody was purchased from Covance (Richmond, CA). Rabbit anti-phospho-ERK1/2 MAPK was purchased from Cell Signaling Technologies Inc. (Danvers, MA). IRDye conjugated goat anti-mouse IgG antibody (IR680) was purchased from LI-COR Biosciences (Lincoln, NE). Donkey anti-rabbit IgG IR800 antibody was purchased from Rockland Immunochemicals Inc. (Gilbertsville, PA). FITC conjugated secondary antibody was purchased from Jackson ImmunoResearch Laboratories Inc. (West Grove, PA). Vectashield mounting medium was purchased from Vector Laboratories (Burlingame, CA). The anti-N-terminal human CB<sub>2</sub> antibody was previously characterized (Benito et al., 2005).

Solutions used in immunocytochemistry, MAPK and internalization assays included:

phosphate buffer (PB: 100 mM NaH<sub>2</sub>PO<sub>4</sub>, pH 7.4), phosphate buffered saline (PBS: 137 mM NaCl, 100 mM NaH<sub>2</sub>PO<sub>4</sub>, 2.7 mM KCl, pH 7.4), HEPES buffered saline (HBS: 130 mM NaCl, 5.4 mM KCl, 1.8 mM MgCl<sub>2</sub>, 10 mM HEPES, pH 7.5), tris-buffered saline (TBS; 137 mM NaCl, 10 mM Tris, pH 7.4) and 4% paraformaldehyde (4% PFA w/v in PB).

For electrophysiological recordings, normal extracellular solution (ECS) contained: 119 mM NaCl, 5 mM KCl, 2 mM CaCl<sub>2</sub>, 1 mM MgCl<sub>2</sub>, 30 mM glucose and 20 mM HEPES, pH to 7.3 with NaOH. For recording barium currents, the ECS contained: 119 mM NaCl, 5 mM KCl, 10 mM BaCl<sub>2</sub>, 1 mM MgCl<sub>2</sub>, 30 mM glucose and 20 mM HEPES. pH to 7.3 with NaOH. To block sodium currents during calcium channel recordings, >200 nM TTX was added to the ECS. 10 μM nifedipine was also added to block L-type calcium channels. The intracellular solution for recording calcium currents contained 100 mM CsCl, 1 mM MgCl<sub>2</sub>, 3 mM MgATP, 0.3 mM LiGTP, 10 mM HEPES, 20 mM phosphocreatine, 10 mM EGTA, 50 units/ml creatine phosphokinase, pH 7.3 with CsOH.

**Cell Culture.** Human Embryonic Kidney (HEK) (catalog #CRL-1573) and AtT20 (catalog #CRL-1795) cells were purchased from American Type Culture Collection (Boston, MA). AtT20 cells used for calcium channel recordings were generously provided by Dr. Gerry Oxford (Indiana University School of Medicine, Indianapolis, IN). AtT20 cell transfection was performed using the Superfect reagent (Qiagen, Valencia,

CA). HEK293 cell transfection was done using the Lipofectamine 2000 reagent (Invitrogen, Carlsbad, CA). Both were conducted according to the manufacturer's instructions. Stable cell lines were made as previously described (Brown et al., 2002; Daigle et al., 2008). Plasmids encoding pplss-HA-rat CB<sub>1</sub>-pcDNA3.0 (rCB<sub>1</sub>), pplss-HA-mouse CB<sub>2</sub>-pcDNA3.0 (mCB<sub>2</sub>), HA-rat CB<sub>2</sub>-pcDNA3.0 (rCB<sub>2</sub>), pplss-HA-human CB<sub>2</sub>-pTRE2 (hCB<sub>2</sub>), human CB<sub>2</sub>-pcDNA3 (untagged hCB<sub>2</sub>), and  $\beta$ -arrestin<sub>2</sub>-mRFP pEF4a were all constructed, amplified and purified using NEB buffers and restriction enzymes (New England BioLabs, Ipswich, MA) and Qiagen plasmid DNA purification kits (Valencia, CA) according to the manufacturer's instructions. The amino-terminal HA (hemagglutinin) epitope tag was added for ease of immunostaining. An amino-terminal preprolactin signal sequence (pplss) was added to enhance cannabinoid receptor surface expression in HEK293 cells (Daigle et al., 2008). The pTRE2 vector was chosen for hCB<sub>2</sub> due to the extremely higher expression levels obtained using hCB<sub>2</sub> in the pcDNA3.0 plasmid. Sequencing was performed to verify each construct's integrity (Indiana University Molecular Biology Institute). Primers for sequencing and cloning were purchased from Operon (Huntsville, AL). Cell lines were grown in Dulbecco's modified Eagle's medium with 10% fetal bovine serum, 100 units/ml penicillin, and 100  $\mu$ g/ml streptomycin. All cells were grown at 37° C in 5% CO<sub>2</sub> humidified air.

**Immunocytochemistry.** HEK293 cells expressing rCB<sub>1</sub> and rCB<sub>2</sub> were treated and immunostained according to the protocols outlined in (Daigle et al., 2008) and (Kearn et al., 2005). Briefly, cells were grown on poly-D lysine coated coverslips in 24 well plates. Cells were washed once with HBS/BSA (HBS + 0.2 mg/ml BSA) and drug treatments

were performed at 37°C with drugs diluted in HBS/BSA. Following drug treatments, cells were fixed with 4% paraformaldehyde, washed and blocked in PBS with 5% DDS and 0.1% saponin (for membrane permeabilization). Primary antibody treatment was performed for 3 hours at room temperature or overnight at 4°C. Cells were washed and secondary antibody incubation was done for 1 hour at room temperature. Finally, cells were washed, dried and mounted on glass slides using Vectashield with DAPI. Cells were visualized using a Nikon Eclipse TE2000E confocal microscope at 60X magnification for internalization experiments and 100X for  $\beta$ -arrestin experiments (Indiana University METACyt facilities).

**Internalization and MAPK assays.** Internalization assays (quantitative on-cell western) were performed as previously described in (Atwood et al., 2010). For internalization experiments using pertussis toxin (PTX), the cells were incubated overnight in PTX (400 ng/ml). For internalization experiments using sucrose (350 mM), URB597 (100 nM) and JZL184 (100 nM), the cells were pre-treated for 20 minutes and the treatment was continued throughout the duration of the experiment. For experiments comparing untagged to HA-tagged receptors, an anti-N-terminal rat CB<sub>2</sub> antibody was used instead of the anti-HA antibody used in all other experiments. At least three replicates for each time point or concentration were performed for each independent experiment.

For MAPK assays (quantitative in-cell system), HEK293 cells stably expressing rCB<sub>1</sub> or rCB<sub>2</sub> were plated to near confluence on poly-D lysine coated 96 well plates (Corning, Corning, NY, USA) in serum-free growth media and incubated over night. Drug

containing solutions were made in the serum-free media and added to the wells at appropriate time points. Following drug incubation the wells were emptied and ice cold 4% PFA was added immediately to each well and the plates were placed on ice for 15 minutes, followed by 30 minutes at room temperature. The PFA was then removed and >100  $\mu$ l of ice-cold methanol was added to each well and the plate was incubated at -20 °C for >15 minutes. An additional washing step was performed using PBS containing 0.1% Triton-X 100 for 25 minutes (5 minute washes x 5). The PBS/Triton-X 100 was replaced with Odyssey blocking buffer and incubated for >1.5 hours at room temperature. The blocking solution was then removed and replaced by blocking solution containing rabbit anti-phospho-ERK1/2 MAPK antibody (1:200) and was shaken overnight at 4 °C or for 2.5 hours at room temperature. The antibody solution was removed and the plates were washed 5 times with TBS containing 0.05% Tween-20 (TBST) for 5 minutes each time. Blocking solution containing a donkey anti-rabbit IgG antibody (1:200 dilution) conjugated with an IR800 dye was added and shaken for 1 hour at room temperature. The plates were then washed 5 times with TBST, 5 minutes each time. The plates were patted dry and then scanned using a LI-COR Odyssey. The amount of MAPK activation and internalization were calculated as the average integrated intensities of the drug treated wells divided by the average integrated intensities of the untreated wells and are expressed as percentages. Three to four replicates were performed for each time point or concentration for each independent experiment.

**$\beta$ -arrestin recruitment assays.** HEK293 cells were transiently transfected with  $\beta$ -

arrestin<sub>2</sub>-mRFP and either HArCB<sub>1</sub> pcDNA3 or HArCB<sub>2</sub> pcDNA3 and plated on to glass coverslips in 24 well dishes. Transient transfection of both receptor and β-arrestin<sub>2</sub> was used as we previously found that stable expression of either the receptor or β-arrestin<sub>2</sub> inhibited expression of the other, whether stably or transiently expressed. Cells were drug-treated for 7 minutes, fixed and CB<sub>1</sub> or CB<sub>2</sub> receptors detected as described above. Images of the fluorescently detected HA11 antibody and mRFP β-arrestin<sub>2</sub> were processed using MetaMorph software (Molecular Devices, Sunnyvale, CA). Line scans of pixel intensity were made across cells that expressed (non-saturating) levels of β-arrestin<sub>2</sub>-mRFP. Line scans of β-arrestin<sub>2</sub>-mRFP and FITC-anti-mouse (the presence of CB<sub>2</sub> receptor defines the cell membrane) were compared to determine the location of the outer cell membrane on the line scan. The average intensity of β-arrestin<sub>2</sub>-mRFP was assessed at this point (within 1 μm of the membrane edge) and divided by the average intensity of mRFP in the cytosol to obtain a membrane:cytosol ratio. Membrane:cytosol ratios greater than 1 were interpreted as membrane recruitment of β-arrestin<sub>2</sub>-mRFP.

**Voltage-gated calcium channel recording.** Calcium channel activity was measured by recording barium currents from wild type untransfected AtT20 cells and AtT20 cells stably expressing rCB<sub>1</sub> or mCB<sub>2</sub> in the whole-cell configuration. The cells were voltage clamped at a holding potential of -70 mV. Voltage-activated currents were evoked by depolarizing the cells to 0 mV for 30 ms from the holding potential every 10 seconds. Currents were measured near the end of each 30 ms voltage step. Cd<sup>2+</sup> insensitive currents were subtracted off-line and the Cd<sup>2+</sup>-sensitive current was taken to be the

barium current flowing through calcium channels. In some experiments we observed linear rundown of barium currents. In these cases we used linear regression analysis to determine the rates of current rundown prior to drug application. Drug effects were determined by measuring the difference between the actual and predicted current based on these rates of rundown.

**Statistical analysis.** Data are reported as mean  $\pm$  SEM (except EC<sub>50</sub>, IC<sub>50</sub> and t<sub>1/2</sub> data are reported as mean  $\pm$  95% confidence interval). Nonlinear regression was used to fit the concentration response curves and the time courses of receptor internalization. Student's t-tests and one-way ANOVA with Bonferroni's multiple comparisons or Dunnett post-tests were used where indicated. Statistical significance is denoted as follows: \*\*\*p<0.0001, \*\*p < 0.01, and \*p < 0.05. All graphs and statistical analyses were generated using GraphPad Prism 4.0 software (Hearne Scientific Software, Chicago, IL). Densitometric analysis was performed using Image J software.

## Results

**Ligand-directed internalization of rCB<sub>1</sub> and rCB<sub>2</sub> receptors in HEK293 cells.** To measure cannabinoid receptor internalization we employed HEK293 cells stably expressing HA-tagged rat CB<sub>1</sub> (rCB<sub>1</sub>) and rat CB<sub>2</sub> (rCB<sub>2</sub>) receptors. In these cells internalization is inversely proportional to receptor level (i.e., the higher the surface levels of the receptor, the lower the maximal internalization). Thus, we utilized stable cell lines with similar surface expression levels (as assessed by quantitative on-cell western analysis (Supplemental Figure 1A: rCB<sub>1</sub>: 1.0  $\pm$  0.05, rCB<sub>2</sub>: 1.1  $\pm$  0.07 (relative



units),  $p = 0.11$ ). However, the rCB<sub>2</sub> cells had a higher total expression level than rCB<sub>1</sub> cells (1.9 fold higher) as assessed by conventional western blot analysis (Supplemental Figure 1B,C). This discrepancy between total protein level and surface level is likely due to the constitutive internalization of CB<sub>2</sub> observed by others, leading to a larger intracellular pool of CB<sub>2</sub> (Bouaboula et al., 1999). Nevertheless, because these two cell lines had nearly identical surface levels under basal conditions, this enabled us to compare internalization due to drug treatments between these two cell lines.

CP55,940 and WIN55,212-2 are widely used and are generally regarded as non-selective, highly potent and efficacious CB<sub>1</sub> and CB<sub>2</sub> receptor agonists (Howlett et al., 2002). Fig. 1A shows the time course of rCB<sub>1</sub> and rCB<sub>2</sub> internalization produced by 100 nM CP55,940. CP55,940 treatment internalizes both rCB<sub>1</sub> and rCB<sub>2</sub> to a similar extent, reaching a plateau of  $56 \pm 3.2\%$  of basal surface levels in rCB<sub>1</sub> expressing cells and  $59 \pm 1.3\%$  in rCB<sub>2</sub> expressing cells. rCB<sub>2</sub> internalized much more rapidly with a half-life of 8.2 minutes (5.6 to 15 min) compared to 36 minutes (24 to 71 min) for rCB<sub>1</sub>. CP55,940 promoted internalization of rCB<sub>1</sub> and rCB<sub>2</sub> (Fig. 1B) with nearly equal potencies (rCB<sub>1</sub>:  $EC_{50} = 0.48$  nM (0.17 to 1.4 nM); rCB<sub>2</sub>:  $EC_{50} = 1.3$  nM (0.68 to 2.3 nM)) and efficacies (rCB<sub>1</sub>:  $E_{max} = 56 \pm 2.0\%$  basal surface levels, rCB<sub>2</sub>:  $E_{max} = 59 \pm 1.2\%$  of basal surface levels). In rCB<sub>1</sub> cells, 100 nM CP55,940-induced internalization could be blocked by 1  $\mu$ M rimonabant, a CB<sub>1</sub> receptor antagonist/inverse agonist (Fig. 1C:  $93 \pm 3.0\%$  of basal surface levels,  $p < 0.001$  vs. CP55,940 alone). For rCB<sub>2</sub> cells, 1  $\mu$ M AM630, a CB<sub>2</sub> receptor antagonist, attenuated internalization by CP55,940 (Fig. 1C:  $83 \pm 1.8\%$  of basal surface levels,  $p < 0.001$  vs. CP55,940 alone). As expected from previous work,

WIN55,212-2 also produced rCB<sub>1</sub> receptor internalization (Fig. 1D) with a maximal internalization of 45 ± 3.4% of basal surface levels and a half-life of 34 (24 to 57) min. Surprisingly, 100 nM WIN55,212-2 did not produce any rCB<sub>2</sub> internalization, even after 180 minutes of treatment (Fig. 1D). This was not a consequence of the concentration used as even 1 μM WIN55,212-2 did not produce rCB<sub>2</sub> internalization (Fig. 1E). 1 μM rimonabant could also prevented 1 μM WIN55,212-2 from internalizing rCB<sub>1</sub> (Fig. 1F: 96 ± 4.8% of basal surface levels, *p* < 0.001 vs. WIN55,212-2 alone). AM630 had no effect on surface CB<sub>2</sub> during WIN55,212-2 treatment (Fig. 1F). Fig. 1G provides representative images of cells treated with 100 nM CP55,940 or WIN55,212-2 for 120 minutes and also co-treatments with antagonists. It is of interest that the pattern of internalization differs between the two cell lines, with rCB<sub>2</sub> internalization resulting in more perinuclear localization of the receptor than for rCB<sub>1</sub>, suggesting that internalized CB<sub>1</sub> and CB<sub>2</sub> may localize to different endosomal compartments. To test whether cannabinoid receptor internalization observed here was dependent on G protein activation, cells were treated over-night with 400 ng/ml *Pertussis* toxin (PTX). PTX did not alter the magnitude (Supplemental Figure 2A) of CP55,940 and WIN55,212-2 induced receptor internalization in either rCB<sub>1</sub> or rCB<sub>2</sub> cells. It also did not alter the kinetics of internalization for rCB<sub>1</sub> (CP55,940: 45 (27 to 145) min; WIN55,212-2: 54 (31 to 192) min) or rCB<sub>2</sub> (CP55,940: 11 (8.0 to 18) min). This suggests that this internalization is independent of G<sub>i/o</sub> G protein activation. Interestingly despite the inability to alter the kinetics or magnitude of agonist-induced receptor internalization, PTX did produce a small, but significant increase in basal receptor surface levels in rCB<sub>1</sub> cells (110 ± 2.2% of basal surface levels, *p* = 0.033 vs. untreated) and a larger

increase in rCB<sub>2</sub> cells ( $130 \pm 1.9\%$  of basal surface levels,  $p < 0.0001$  vs. untreated), suggesting that G<sub>i/o</sub> G protein activation may play a role in basal cannabinoid receptor trafficking (Supplemental Figure 2C). To determine whether or not the internalization we observed in these cells was clathrin-mediated, we treated these cells with CP55,940 and WIN55,212-2 in the presence of 350 mM sucrose, which blocks clathrin-mediated endocytosis (Hsieh et al., 1999). Sucrose completely prevented CP55,940-induced internalization of both rCB<sub>1</sub> and rCB<sub>2</sub> (Supplemental Figure 2A: rCB<sub>1</sub>:  $96 \pm 1.1\%$  of basal surface levels,  $p < 0.001$  vs. CP55,940 alone; CB<sub>2</sub>:  $93 \pm 2.8\%$  of basal surface levels,  $p < 0.001$  vs. CP55,940 alone), and rCB<sub>1</sub> internalization due to WIN55,212-2 treatment (Supplemental Figure 2B:  $93 \pm 3.8\%$  of basal surface levels,  $p < 0.001$  vs. WIN55,212-2 alone). Sucrose alone did not significantly alter rCB<sub>1</sub> surface levels, but produced a small, yet statistically significant increase in rCB<sub>2</sub> surface levels ( $110 \pm 0.77\%$  of basal levels,  $p = 0.010$ ) (Supplemental Figure 2C).

There have been reports that rCB<sub>2</sub>, mCB<sub>2</sub> and hCB<sub>2</sub> receptors possess significantly different pharmacological profiles despite each being a CB<sub>2</sub> receptor (Bingham et al., 2007; Mukherjee et al., 2004). Thus, the effect of WIN55,212-2 observed above may be unique to the rat CB<sub>2</sub> receptor. Furthermore the cellular environment may also be a contributing factor. To test these possibilities we treated HEK293 cells expressing mCB<sub>2</sub> or hCB<sub>2</sub> receptors as well as AtT20 cells expressing rCB<sub>2</sub> or mCB<sub>2</sub> receptors with CP55,940 or WIN55,212-2 (Supplemental Figure 3A). In all cell lines we obtained a similar pattern of results as we observed in our rCB<sub>2</sub> HEK293 cells. 100 nM CP55,940 promoted CB<sub>2</sub> receptor internalization in each cell line, whereas 1  $\mu$ M WIN55,212-2

produced little if any internalization. The effect of CP55,940 could be significantly inhibited by a co-treatment with 1  $\mu$ M SR144528 in all cell lines and by 1  $\mu$ M AM630 in the rCB<sub>2</sub> AtT20 cell lines and all the HEK293 cell lines. AM630 attenuated the effects of CP55,940 in the mCB<sub>2</sub> AtT20 cell line, but this difference did not reach statistical significance. This is likely due to the high expression level of mCB<sub>2</sub> in these cells, which may also account for the reduced effectiveness of CP55,940 in promoting receptor internalization in these cells. Nonetheless, the general pharmacological pattern is consistent across all cell lines.

It is also a possibility that the lack of internalization observed here for WIN55,212-2 was due to the presence of the HA-epitope tag found on the N-terminus of the CB<sub>2</sub> receptors. To determine this we measured receptor internalization induced by CP55,940 and WIN55,212-2 of untagged hCB<sub>2</sub> stably expressed in HEK293 cells. In these experiments we used an antibody directed towards the N-terminus of CB<sub>2</sub>. We observed similar results as with the HA-tagged receptors: CP55,940 promoted internalization of the untagged CB<sub>2</sub> receptor ( $74 \pm 5.1\%$  of basal surface levels) and WIN55,212-2 was ineffectual ( $100 \pm 3.8\%$  of basal surface levels) (Supplemental Figure 3B). Taken together, these data suggest that the results we obtained in our internalization experiments are not limited to a specific cell type, species of CB<sub>2</sub> or the presence of an epitope tag.

Since we found such a profound difference between two ligands that are widely considered to be interchangeable CB<sub>2</sub> agonists, we expanded our study to include a

range of cannabinoid receptor ligands. Fig. 2 provides the concentration response curves following 2 hours of treatment with each of these ligands, grouped by ligand family. Supplemental Table 1 provides a summary of the data displayed in Fig. 2, giving  $EC_{50}$ 's and maximal internalization achieved. For all ligands that produced internalization, we also determined efficacy of antagonist block using 1  $\mu$ M rimonabant for rCB<sub>1</sub> and 1  $\mu$ M AM630 for rCB<sub>2</sub> cells. For all ligands we found that rimonabant could significantly block internalization in rCB<sub>1</sub> cells and AM630 in rCB<sub>2</sub> cells (Supplemental Figure 4). Fig. 2A details the effects of aminoalkylindoles, the same class of ligand to which WIN55,212-2 belongs. Interestingly, all aminoalkylindoles tested produced modest to no internalization of rCB<sub>2</sub> receptors (Figure A2) and AM1241, reported to be a CB<sub>2</sub> selective agonist, slightly increased surface levels of rCB<sub>2</sub>. JWH015, frequently used as a "CB<sub>2</sub>-selective agonist" significantly internalized rCB<sub>1</sub> (Fig. 2A1). This was markedly greater than the internalization produced in rCB<sub>2</sub> cells ( $p = 0.0015$ ). THC did not produce any rCB<sub>2</sub> internalization, but JWH133, THCV and HU210 did, despite being structurally similar to THC. The iminothiazole compound, A-836339, potently produced moderate rCB<sub>2</sub> internalization as did the cannabilactone AM1710 (Fig. 2D2) (Rahn et al., 2011). A-836339 also produced extensive rCB<sub>1</sub> internalization, but its  $EC_{50}$  for rCB<sub>1</sub> internalization was about 800-fold higher than that for rCB<sub>2</sub>. AM1710 and JWH133 were the only compounds that produced greater internalization of rCB<sub>2</sub> than rCB<sub>1</sub>. We also confirmed that SR144528 increased surface levels of CB<sub>2</sub> (Bouaboula et al., 1999), but interestingly, AM630, a structurally distinct CB<sub>2</sub> receptor antagonist did not significantly increase cell surface CB<sub>2</sub> (Fig. 2E2). Rimonabant had no effect on either rCB<sub>1</sub> or rCB<sub>2</sub> surface levels (Supplemental Table 1).

As shown in Fig. 2C1, the endocannabinoids 2-AG and AEA produced some internalization in rCB<sub>1</sub> cells, albeit at very high concentrations. This may be due to the low intrinsic activity of these ligands for internalization or due to endocannabinoid breakdown via catabolic enzymes endogenously expressed in HEK293 cells. Fatty acid amide hydrolase (FAAH) is the enzyme primarily responsible for breakdown of anandamide (Cravatt et al., 2001; Ligresti et al., 2005), while monoacylglycerol lipase (MGL) is reported to be the enzyme that is primarily responsible for the degradation of 2-AG, although other enzymes contribute (Blankman et al., 2007). HEK293 cells possess significant levels of mRNA (as assessed by microarray analysis) for enzymes involved in endocannabinoid synthesis and degradation including FAAH (Supplemental Figure 5A). We detected MGL mRNA, but at a statistically insignificant level, although other enzymes that may degrade 2-AG were detected at significant levels ( $\alpha/\beta$ -hydrolases 6 and 12). URB597, a selective inhibitor of FAAH, effectively increased the ability of low concentrations of AEA to promote rCB<sub>1</sub> internalization (Supplemental Figure 5B) but had little effect on rCB<sub>2</sub> internalization (Supplemental Figure 5C). 100 nM URB597 treatment shifted the EC<sub>50</sub> of AEA-mediated rCB<sub>1</sub> internalization from 1.5  $\mu$ M (0.1 to 16  $\mu$ M) to 64 nM (13 to 320 nM). Maximal internalization was not significantly increased (30  $\mu$ M AEA: 69  $\pm$  4.7% basal surface levels; 30  $\mu$ M AEA + 100 nM URB597: 56  $\pm$  3.4% of basal surface levels). JZL184, an inhibitor of MGL (Long et al., 2009), did not produce a shift in the concentration response curves for either rCB<sub>1</sub> or rCB<sub>2</sub> (Supplemental Figures 5B and 5C).

### **WIN55,212-2 competitively antagonizes agonist-induced rCB<sub>2</sub> receptor**

**internalization.** Since CP55,940 produced robust rCB<sub>2</sub> internalization and WIN55,212-2 produced no internalization, it is possible that WIN55,212-2 could competitively antagonize CP55,940 internalization. Fig. 3A shows a time course of rCB<sub>2</sub> internalization produced by treatment with 100 nM CP55,940 alone or with increasing concentrations of WIN55,212-2 as a co-treatment. WIN55,212-2 prevents CP55,940-induced rCB<sub>2</sub> internalization and this was concentration dependent. The same was not true for rCB<sub>1</sub> cells where WIN55,212-2 (100 nM or 1  $\mu$ M) had no effect on the internalization induced by 100 nM CP55,940 (Fig. 3B). Fig. 3C shows representative images of rCB<sub>1</sub> or rCB<sub>2</sub> cells co-treated with 100 nM CP55,940 and 1  $\mu$ M WIN55,212-2. To further explore the concentration dependence of this effect, we performed two complementary experiments with rCB<sub>1</sub> and rCB<sub>2</sub> cells. First, we applied a constant 100 nM CP55,940 with co-treatments of increasing concentrations of WIN55,212-2. WIN55,212-2 concentration-dependently reduced CP55,940-induced internalization in rCB<sub>2</sub> cells, but not in rCB<sub>1</sub> cells (Fig. 3D). We then repeated the experiment, but this time with a constant 100 nM WIN55,212-2 and increasing concentrations of CP55,940 (Fig. 3D). Increasing concentrations of CP55,940 overcame the antagonistic effect of WIN55,212-2 on rCB<sub>2</sub> internalization, but had no effect on rCB<sub>1</sub> internalization. To further explore the mechanistic basis of the antagonistic effect of WIN55,212-2 we performed the same experiment as above: a fixed concentration of WIN55,212-2 with increasing concentrations of CP55,940 over a wide range of concentrations of WIN55,212-2 as a co-treatment. As seen in Fig. 3E, increasing concentrations of WIN55,212-2 shifted the CP55,940 concentration curve to the right as would a rCB<sub>2</sub>

antagonist. We constructed a Schild plot of these data (Fig. 3F) to determine whether the antagonistic effect of WIN55,212-2 was competitive in nature. The slope of the line obtained in the Schild plot analysis was  $0.98 \pm 0.065$ , suggesting that WIN55,212-2 competitively antagonizes CP55,940-induced rCB<sub>2</sub> internalization. WIN55,212-2 was also able to block CP55,940 induced CB<sub>2</sub> internalization in both HEK293 and AtT20 cells and in cells expressing mCB<sub>2</sub> and hCB<sub>2</sub> (Supplemental Figure 3A). This once again suggests that the effects of WIN55,212-2 are not unique to rCB<sub>2</sub> or HEK293 cells. WIN55,212-2 was also not unique in its ability to prevent CP55,940-induced rCB<sub>2</sub> internalization. Fig. 3G shows data obtained using 10 nM CP55,940 and co-treatments with 100 nM and 1  $\mu$ M of other ligands. Other ligands from the same aminoalkylindole class as WIN55,212-2 (AM1241 and JWH015) also antagonized CP55,940-induced internalization. AM1241 was more potent of an antagonist than JWH015. THC, a low efficacy CB<sub>2</sub> agonist in most assays, also antagonized CP55,940-induced rCB<sub>2</sub> internalization. Other classical cannabinoids, THCV and JWH133 had little to no effect on CP55,940's ability to promote rCB<sub>2</sub> internalization. The CB<sub>2</sub> antagonists AM630 and SR144528 blocked internalization as expected. The endocannabinoid 2-AG had no effect. A-836339 also could antagonize the internalization obtained using CP55,940, consistent with its high affinity for CB<sub>2</sub>, but low efficacy to promote internalization (Fig. 2D). AM1710 had no effect. Thus it appears that WIN55,212-2, other aminoalkylindoles, and some low internalizing CB<sub>2</sub> ligands, such as THC and A-836339, all can antagonize CP55,940-induced rCB<sub>2</sub> internalization.



**WIN55,212-2 engages rCB<sub>2</sub> to activate specific signaling pathways: evidence for functional selectivity.** Following these experiments demonstrating that WIN55,212-2 not only failed to promote rCB<sub>2</sub> internalization, but actually antagonized it, we were concerned whether WIN55,212-2 was capable of activating rCB<sub>2</sub> in our cell lines. To test this possibility we performed two different types of experiments. First we tested whether CP55,940 and WIN55,212-2 could activate ERK1/2 (p42/44) MAPK. Second, we analyzed the ability of these two compounds to promote  $\beta$ -arrestin<sub>2</sub> recruitment in cells co-expressing rCB<sub>2</sub> (or rCB<sub>1</sub> as a control) and  $\beta$ -arrestin<sub>2</sub>.

We used the same cell lines that were used for the internalization assays to measure levels of phospho-ERK1/2. In rCB<sub>1</sub> HEK293 cells, ERK1/2 activation was maximal following 5 minutes of treatment (Fig. 4A) for both 100 nM CP55,940 ( $220 \pm 8.7\%$  of basal levels) and 100 nM WIN55,212-2 ( $200 \pm 7.6\%$  of basal levels). There was a significant difference in the amount of MAPK activation achieved by each drug treatment only at 5 minutes ( $p = 0.043$ ). We repeated this time course experiment with rCB<sub>2</sub> HEK293 cells and found that both 100 nM CP55,940 and WIN55,212-2 could activate MAPK (Fig. 4B). Interestingly, CP55,940 reached maximal activation at 5 minutes of treatment ( $160 \pm 2.4\%$  of basal levels) similar to the timing of the peak in rCB<sub>1</sub> cells, but WIN55,212-2 produced a somewhat more prolonged activation than CP55,940, reaching a peak between 5 and 7.5 minutes (5 minutes:  $140 \pm 3.5\%$  of basal levels; 7.5 minutes:  $140 \pm 3.4\%$  of basal levels, ns). CP55,940 and WIN55,212-2 activated ERK1/2 in rCB<sub>1</sub> HEK293 cells in a concentration dependent manner with CP55,940 being significantly more potent ( $EC_{50} = 1.4$  nM (0.56 to 3.3 nM)) than

WIN55,212-2 ( $EC_{50} = 19$  nM (9.0 to 40 nM)) (Fig. 4C). We found no differences in maximal efficacies (CP55,940:  $E_{max} = 220 \pm 5.2\%$  of basal levels; WIN55,212-2:  $E_{max} = 220 \pm 6.9\%$  of basal levels). In  $rCB_2$  cells, treatments with both compounds resulted in MAPK activation that was also concentration dependent (Fig. 4D). CP55,940 was somewhat more potent than WIN55,212-2 (CP55,940:  $EC_{50} = 0.56$  nM (0.18 to 22 nM); WIN55,212-2:  $EC_{50} = 2.6$  nM (0.49 to 13 nM)). CP55,940 was significantly more efficacious (CP55,940:  $E_{max} = 150 \pm 2.3\%$  of basal levels) than WIN55,212-2 ( $E_{max} = 140.0 \pm 2.5\%$  of basal levels). In  $rCB_1$  cells 1  $\mu$ M rimonabant inhibited the effects of 100 nM CP55,940 (Fig. 4C:  $102 \pm 7.0\%$  of basal levels,  $p < 0.0001$  vs. CP55,940 alone) and 100 nM WIN55,212-2 ( $94 \pm 6.4\%$  of basal levels,  $p < 0.0001$  vs. WIN55,212-2 alone) and 1  $\mu$ M AM630 did the same in  $rCB_2$  cells (Fig. 4D:  $120 \pm 6.0\%$  of basal levels,  $p < 0.0001$  vs. CP55,940;  $99 \pm 1.0\%$  of basal levels,  $p < 0.0001$  vs. WIN55,212-2). Receptor-independent activation of ERK1/2 MAPK using phorbol 12-myristate 13-acetate (PMA) resulted in much higher levels of MAPK activation ( $rCB_1$ :  $420 \pm 84\%$  of basal;  $rCB_2$ :  $400 \pm 29\%$ ; native HEK293 cells:  $380 \pm 22\%$ ) demonstrating that the maximal effects by WIN55,212-2 and CP55,940 were non-saturating (Supplemental Figure 6). CP55,940 and WIN55,212-2 had no effect on ERK1/2 phosphorylation in untransfected HEK293 cells (CP55,940:  $100 \pm 2.2\%$  basal; WIN55,212-2:  $100 \pm 3.7\%$  basal).

We next looked at  $\beta$ -arrestin membrane recruitment as an indicator of receptor activation.  $\beta$ -arrestins are proteins that are recruited to activated GPCRs and prevent the association of the activated receptor with its G proteins and later may serve as

scaffolds to recruit signaling complexes to the GPCR ((Rajagopal et al., 2010)).  $\beta$ -arrestin recruitment can be observed as a redistribution of fluorescently-labeled  $\beta$ -arrestin from the cytosol to the membrane following drug treatment and has been characterized in rCB<sub>1</sub> expressing HEK293 cells (Daigle et al., 2008). To determine whether  $\beta$ -arrestin translocated in this manner in response to CP55,940 and WIN55,212-2, we transiently transfected HEK293 cells with either rCB<sub>1</sub> or rCB<sub>2</sub> and  $\beta$ -arrestin<sub>2</sub> with a mRFP tag. Fig. 5A shows HEK293 cells that express rCB<sub>1</sub> (bottom panels) and  $\beta$ -arrestin<sub>2</sub>-mRFP (top panels) after various treatments. Following treatment with either 100 nM CP55,940 or 100 nM WIN55,212-2,  $\beta$ -arrestin<sub>2</sub>-mRFP moved from a predominately cytosolic distribution (Fig. 5A1) to a more membrane-associated distribution (Figs. 5A2 and 5A4 respectively). This effect could be prevented by 1  $\mu$ M rimonabant (Figs. 5A3 and 5A5). Fig. 5C quantifies the data obtained with these rCB<sub>1</sub> expressing cells. The basal membrane/cytosol ratio was  $0.91 \pm 0.038$ . 100 nM CP55,940 significantly promoted  $\beta$ -arrestin<sub>2</sub> membrane recruitment, increasing the membrane/cytosol ratio to  $1.3 \pm 0.060$  ( $p < 0.001$  vs. untreated) as did 100 nM WIN55,212-2 ( $1.4 \pm 0.10$ ,  $p < 0.001$  vs. untreated). Rimonabant prevented this recruitment for both CP55,940 ( $0.83 \pm 0.050$ ,  $p < 0.001$  vs. CP55,940) and WIN55,212-2 ( $0.96 \pm 0.050$ ,  $p < 0.001$  vs. WIN55,212-2). Repeating this experiment, but this time with HEK293 cells transiently expressing rCB<sub>2</sub> instead of rCB<sub>1</sub>, we obtained similar results. Of interest, even in untreated rCB<sub>2</sub> cells, a substantial fraction of  $\beta$ -arrestin<sub>2</sub> was already at the membrane (Figs. 6B1 and 6C, membrane:cytosol ratio:  $1.15 \pm 0.060$ ). This is likely due to constitutive activity of CB<sub>2</sub> as noted by others in CB<sub>2</sub> overexpressing cells (Bouaboula et al., 1999). However, despite the basal membrane localization, 100 nM

CP55,940 significantly increased membrane recruitment (Figs. 5B2 and 5C;  $2.1 \pm 0.15$   $p < 0.001$  vs. untreated). AM630 attenuated this effect (Figs. 5B3 and 5C:  $1.5 \pm 0.12$   $p < 0.01$  vs. CP55,940, ns vs. untreated).  $1 \mu\text{M}$  WIN55,212-2 promoted significant translocation of  $\beta$ -arrestin<sub>2</sub> from the cytosol to the membrane in rCB<sub>2</sub> cells (Figs. 5B4 and 5C:  $1.6 \pm 0.090$ ,  $p < 0.05$  vs. untreated) and this was significantly inhibited by  $1 \mu\text{M}$  AM630 (Figs. 6B5 and 6C,  $0.95 \pm 0.050$ ,  $p < 0.001$  vs. WIN55,212-2, ns vs. untreated). Thus, although less potent than CP55,940, WIN55,212-2 is capable of activating rCB<sub>2</sub> to promote  $\beta$ -arrestin<sub>2</sub> membrane recruitment. Control experiments with HEK293 cells expressing only  $\beta$ -arrestin<sub>2</sub> did not reveal any effect of  $1 \mu\text{M}$  WIN55,212-2,  $100 \text{ nM}$  CP55,940,  $1 \mu\text{M}$  AM630 or  $1 \mu\text{M}$  rimonabant on membrane localization of  $\beta$ -arrestin<sub>2</sub> (Fig. 5C:  $p = 0.28$ ). This suggests that the effects seen with these drugs are indeed due to cannabinoid receptor activation and not due to activation of other GPCRs that might be present in HEK293 cells. These two sets of results ( $\beta$ -arrestin and MAPK) convinced us that WIN55,212-2 is capable of activating rCB<sub>2</sub> and suggested that WIN55,212-2 may display functional selectivity with respect to internalization.

**CB<sub>2</sub>-mediated inhibition of voltage gated calcium channels: further evidence that WIN55,212-2 is a functionally selective CB<sub>2</sub> ligand.** Early studies reported that CB<sub>2</sub> does not effectively modulate voltage gated calcium or G protein-regulated potassium channels (Felder et al., 1995; Ross et al., 2001). However, these studies employed WIN55,212-2 as the CB<sub>2</sub> agonist. Based on our internalization data, we hypothesized that WIN55,212-2 is a poor agonist at CB<sub>2</sub> in regard to inhibition of voltage gated calcium channels (VGCCs). We revisited the calcium channel experiments done in

AtT20 cells (Felder et al., 1995), comparing the effectiveness of WIN55,212-2 and CP55,940. For these experiments we employed the mCB<sub>2</sub> expressing AtT20 cells used in Supplemental Figure 3A. We also used wild-type, untransfected AtT20 cells and rCB<sub>1</sub> expressing AtT20 cells as controls. Figs. 6A and 6D show that 100 nM and 1 μM WIN55,212-2 failed to inhibit VGCCs in mCB<sub>2</sub> expressing AtT20 cells ( $0.4 \pm 1.6\%$  and  $-3.4 \pm 3.2\%$  inhibition respectively). In contrast, 100 nM WIN55,212-2 inhibited VGCCs in rCB<sub>1</sub> expressing AtT20 cells ( $13 \pm 3.8\%$  inhibition) (Fig. 6E). 100 nM CP55,940, as seen in Figs. 6B and 6D, reduced the magnitude of barium currents in mCB<sub>2</sub> expressing cells in a concentration dependent fashion ( $IC_{50} = 18 \text{ nM}$  (1.1 to 290.0 nM),  $E_{max} = 18 \pm 2.2\%$  inhibition). Inhibition by 100 nM CP55,940 was blocked by 1 μM AM630 treatment ( $4.4 \pm 2.7\%$  activation) and was absent in untransfected wild-type cells ( $0.10 \pm 3.1\%$  inhibition) (Fig. 6E). Interestingly, on its own 1 μM AM630 treatment significantly increased the magnitude of barium currents relative to control (Figs. 6C and 6E:  $12 \pm 2.4\%$  activation, not significantly different from CP55,940 + AM630), thus AM630 acts as an inverse agonist. 100 nM CP55,940 also inhibited VGCCs in rCB<sub>1</sub> expressing cells ( $13 \pm 3.8\%$  inhibition) (Fig. 6E). The effects of CP55,940 in rCB<sub>1</sub> and mCB<sub>2</sub> expressing cells was not statistically different. Supporting the inverse agonist effect of AM630, we found that oxotremorine-m, a muscarinic receptor agonist, was much more effective at inhibiting VGCCs in WT ( $16 \pm 4.3\%$  inhibition) than in mCB<sub>2</sub> expressing AtT20 cells ( $6.5 \pm 1.8\%$ ,  $p = .025$  vs. rCB<sub>1</sub>,  $p = 0.055$  vs. WT) (Fig. 6E), suggesting a constitutive inhibition of VGCC by CB<sub>2</sub>, similar to the data presented in Felder et al., 1995. We also tested whether WIN55,212-2 could block the effects of CP55,940 as it did in our internalization studies. When 100 nM CP55,940 was applied in the presence of 1 μM

WIN55,212-2, CP55,940 did not produce substantial inhibition ( $3.4 \pm 4.3\%$  inhibition,  $p = 0.29$  vs. WIN55,212-2 alone). These data demonstrate another instance of WIN55,212-2 acting as a functional antagonist of CP55,940 at CB<sub>2</sub>.

**Other cannabinoid ligands display functional selectivity at CB<sub>2</sub>.** Based on the differences we observed between CP55,940 and WIN55,212-2 we sought to determine if other cannabinoid ligands also demonstrated functional selectivity. Table 1 compares the efficacies of a select group of cannabinoid ligands in their abilities to activate ERK1/2 MAPK, promote  $\beta$ -arrestin<sub>2</sub>-mRFP membrane recruitment and inhibit VGCCs. Also included in Table 1 is data from Figs. 1 and 2 to allow comparisons between the abilities of these CB<sub>2</sub> ligands to promote internalization with their abilities to act on these other signaling pathways.

Due to the variable nature of the MAPK and  $\beta$ -arrestin recruitment experiments, we again tested CP55,940 and WIN55,212-2 for side-by-side comparisons to the other ligands. For MAPK experiments we compared the levels of phospho-ERK1/2 activation obtained following 5 minutes of treatment with each ligand (Table 1). The effects of the ligands on MAPK in rCB<sub>2</sub> expressing HEK293 cells were compared to those on native HEK293 cells. We found that 2-AG, CP55,940 and WIN55,212-2 were the most efficacious CB<sub>2</sub> ligands in activation of ERK1/2. In contrast, AM1241, AM630 and SR144528 did not significantly affect phospho-ERK1/2 levels in rCB<sub>2</sub> HEK293 cells. We next tested the ability of these same ligands to promote  $\beta$ -arrestin<sub>2</sub> membrane recruitment in CB<sub>2</sub>-expressing cells (Table 1). Interestingly, in this set of experiments

we did not see the basal level of  $\beta$ -arrestin<sub>2</sub> membrane recruitment that we previously saw ( $0.95 \pm 0.024$  membrane/cytosol ratio). However, we still observed robust membrane recruitment in response to CP55,940. We also saw recruitment following treatment with JWH133, AM1710 and A-836339. Each produced significantly more membrane recruitment of  $\beta$ -arrestin<sub>2</sub>-mRFP than observed in untreated cells. No other ligand treatment induced significant levels of  $\beta$ -arrestin<sub>2</sub> membrane recruitment, though the effect of WIN55,212-2 was significantly blocked by AM630 ( $p=0.020$ ). Finally we tested if these ligands would inhibit VGCCs in the mCB<sub>2</sub> expressing AtT20 cells used in Supplemental Figure 3A with native AtT20 cells used as controls (Table 1).

Interestingly, we found that 2-AG was more efficacious than CP55,940 in inhibiting VGCCs. 2-AG did inhibit VGCC's in untransfected AtT20 cells ( $5.9 \pm 1.4\%$  inhibition), however this effect was significantly less than in transfected AtT20 cells ( $p = 0.016$ ). JWH133 and A-836339 also produced inhibition that was significantly greater than that of control. Interestingly, like AM630 (Figs. 6C and 6E), several other ligands acted as inverse agonists, increasing, rather than decreasing, VGCC activity. JWH015 had a minor inverse agonist effect on VGCC activity that was significantly different than that of control ( $p = 0.023$ ) due to its inhibitory effect in non-transfected AtT20 cells ( $4.6 \pm 0.60\%$  inhibition). THCV produced the largest increase, though it was not statistically different from control ( $p = 0.17$ ). THCV was followed by the CB<sub>2</sub> antagonists/inverse agonists AM630 and SR144528. Inverse agonism implies that CB<sub>2</sub> here is constitutively inhibiting VGCCs, either because ongoing synthesis of endogenous ligand or a substantial fraction of the CB<sub>2</sub> receptors are active. Due to a recent report that demonstrated that GW405833 produced CB<sub>2</sub>-dependent behavioral effects when

infused into the nucleus accumbens (Xi et al., 2011), we also tested this compound to determine if its actions could be mediated by inhibition of VGCCs. GW405833 did not produce substantial inhibition of VGCCs (Table 1). These data further suggest that CB<sub>2</sub> is indeed able to couple to VGCCs and that this coupling is highly ligand-dependent.

## Discussion

We began this study focusing on internalization of CB<sub>2</sub> receptors. From our data we conclude that different classes of cannabinoid ligands differ substantially in their ability to promote CB<sub>2</sub> receptor internalization. Non-classical cannabinoids such as CP55,940 and CP47,497-C8 (a synthetic cannabinoid found in "Spice" (Atwood et al., 2011)) are the most efficacious class of cannabinoid ligands for internalization (Figs. 1 and 2, Supplemental Table 1). The aminoalkylindoles (WIN55,212-2, AM1241, JWH015 and JWH018) are the least effective (Figs. 1, 2, Supplemental Table 1). It may be generalized that bicyclic cannabinoids are effective internalizers of CB<sub>2</sub>, whereas aminoalkylindoles are poor internalizers. AM1241 was nearly ineffective as a CB<sub>2</sub> agonist in our other assays as well. However, the AM1241 in this study was a mixture of different stereoisomers and studied primarily on rodent CB<sub>2</sub> receptors. AM1241 produces diverse stereoisomer-specific effects at rodent and human CB<sub>2</sub> receptors (Bingham et al., 2007). The other classes of cannabinoid ligands have a range of efficacy for CB<sub>2</sub> internalization. THC produced no rCB<sub>2</sub> internalization, whereas the other classical cannabinoids tested here produced a moderate amount of internalization. HU-308, another classical cannabinoid, has also been reported to internalize CB<sub>2</sub> in HEK293 cells (Grimsey et al., 2011). The differences between THC



and the other classical cannabinoids tested here parallel THC's weak ability to activate CB<sub>2</sub> (Bayewitch et al., 1995) and the greater efficacies of the other compounds (Bolognini et al. 2010; Howlett et al., 2002). The same may be said of AEA's inability to produce rCB<sub>2</sub> internalization, even in the presence of FAAH inhibitors. AEA is a weak partial agonist at CB<sub>2</sub> in many signaling pathways (Bayewitch et al., 1995). The lack of increased internalization following inhibition of MGL in both rCB<sub>1</sub> and rCB<sub>2</sub> cells suggests that either 2-AG degradation is not responsible for its low potency or that 2-AG metabolism in HEK293 cells may be mediated by hydrolases such as  $\alpha/\beta$ -hydrolases 6 or 12 (Blankman et al., 2007) rather than by MGL. Supporting this latter hypothesis, microarray analysis indicates that HEK293 cells possess significant levels of  $\alpha/\beta$ -hydrolases 6 and 12, but not MGL, mRNA (Supplemental Table 5).

We were surprised that WIN55,212-2 did not produce receptor internalization. WIN55,212-2 is frequently used as a CB<sub>2</sub> receptor agonist. For example, WIN55,212-2 inhibits forskolin-stimulated cAMP accumulation in cannabinoid receptor-expressing HEK293 cells, where it is equally efficacious at CB<sub>2</sub> and CB<sub>1</sub>, but is 10 fold less potent at CB<sub>2</sub> (Tao and Abood, 1998). We expected that since WIN55,212-2 robustly internalizes CB<sub>1</sub> (Atwood et al. 2011, 2010; Hsieh et al., 1999) and is reported as an efficacious agonist at CB<sub>2</sub> (Howlett et al., 2002), that it too would promote significant CB<sub>2</sub> receptor internalization. Not only did WIN55,212-2 not internalize CB<sub>2</sub>, it competitively antagonized internalization by CP55,940. Nonetheless, WIN55,212-2 still activated CB<sub>2</sub> as evidenced by its effects on ERK1/2 and  $\beta$ -arrestin<sub>2</sub>. Our data are consistent with previous studies that found no inhibition of VGCCs by WIN55,212-2

(Felder et al., 1995; Ross et al., 2001). In contrast CP55,940 inhibited VGCC's (Fig. 6). Similar to the internalization assays (Fig. 3), WIN55,212-2 also antagonized inhibition of VGCC's by CP55,940 (Fig. 6F). The data from Fig. 6 clearly indicate that CB<sub>2</sub> will inhibit VGCCs, but that WIN55,212-2 does not activate CB<sub>2</sub> receptors in an appropriate fashion to elicit inhibition. The results reported here examining WIN55,212-2's effects on CB<sub>2</sub> receptor internalization, ERK1/2, β-arrestin and VGCCs imply that WIN55,212-2 shows marked functionally selectivity at CB<sub>2</sub> whereas CP55,940 is less selective.

Functional selectivity (also known as "biased agonism" and "ligand-directed trafficking") is the pharmacological concept that agonists for a particular receptor may selectively and differentially activate specific downstream signaling pathways (Urban et al., 2007). A few studies have examined functional selectivity at CB<sub>2</sub> receptors. One examined CP55,940, 2-AG and 2-AGE functional selectivity using MAPK activation, stimulation of calcium transients and inhibition of adenylyl cyclase as the signaling pathways (Shoemaker et al., 2005). Each ligand differed in its rank order of potency in the three assays despite similar efficacies. Schuehly et al. recently described a case of functional selectivity of CB<sub>2</sub> ligands (Schuehly et al., 2011). AM630 displayed inverse agonist/antagonist actions on CB<sub>2</sub>-mediated inhibition of cAMP production and was silent in its effects on intracellular calcium transients. On the other hand a novel CB<sub>2</sub> ligand, 4'-O-methylhonokiol, was an inverse agonist/antagonist in regards to cAMP production, but potentiated the effects of 2-AG on calcium transients. Our data extend these findings demonstrating that specific CB<sub>2</sub> ligands activate a limited repertoire of signaling pathways. CP55,940 is a broad "agonist" in the classical sense in that it is

highly efficacious across all cellular signaling pathways studied here. SR144528 behaved as an inverse agonist in the internalization assays, increasing surface levels, whereas AM630 didn't, behaving as a neutral antagonist (Fig. 2E2 and Supplemental Table 1). In other assays these two ligands act similarly (Table 1). These observations emphasize that the concept of functional selectivity also applies to inverse agonists, as both compounds are similarly effective inverse agonists in GTP $\gamma$ S binding assays (Ross et al., 1999). These data also support the differences (Schuehly et al., 2011) observed between SR144528 and AM630. However, the lack of effect of AM630 on CB<sub>2</sub> surface levels appears to contradict the Grimsey et al. (2011) report, for unclear reasons. Other ligands also displayed functional selectivity in the different signaling pathways studied here. For example, AM1710 robustly internalized CB<sub>2</sub> and recruited  $\beta$ -arrestin<sub>2</sub>, but weakly activated MAPK and didn't affect VGCC .

Our results provide strong evidence for functional selectivity with respect to internalization among diverse CB<sub>2</sub> receptor agonists. The internalization data presented here is consistent with results from other receptors, such as mu opioid receptors, which have high and low internalizing agonists (Koch and Holtt, 2008; Whistler et al., 1999). Internalization and desensitization of CB<sub>1</sub> appear to be inversely correlated (Wu et al., 2008). If this holds true for CB<sub>2</sub> we hypothesize that WIN55,212-2 and other aminoalkylindoles will rapidly desensitize CB<sub>2</sub> as they produce little receptor internalization. In contrast, agonists that promote CB<sub>2</sub> internalization may cause less desensitization. These data may allow for the development of clinically useful, slowly desensitizing CB<sub>2</sub> agonists .

Rat CB<sub>2</sub> and mouse CB<sub>2</sub> can respond differently than human CB<sub>2</sub> to the same ligands (Bingham et al., 2007), thus it was important to determine if the results were specific to rat CB<sub>2</sub>. Additional data suggest that WIN55,212-2, JWH015, 2-AG and AEA are more human-preferring ligands, whereas CP55,940 shows less selectivity (Mukherjee et al., 2004). There are also two isoforms of rCB<sub>2</sub>, one short—similar to mouse and human CB<sub>2</sub> (Griffin et al., 2000)—and one long (Brown et al., 2002). The studies here used the latter. Based on the data in Supplemental Table 3, agonist differences are much more marked than species differences. Also, the cellular environment in which the receptor is expressed does not appear to determine the pharmacological pattern of internalization we observed, although exceptions may exist for other signaling pathways (Aramori et al., 1997). We expect that CP55,940 and WIN55,212-2 will display similar functional selectivity in cells where CB<sub>2</sub> is natively expressed, though this remains to be determined.

Our results have significant implications for drug development as well as the design and interpretation of experiments studying pharmacological responses to CB<sub>2</sub> agonists. CB<sub>2</sub> agonists show substantial efficacy in multiple preclinical models, including models examining analgesia, inflammation, neuroprotection, anxiety, and ischemia/reperfusion injury. However, to date, the translation of these studies to effective CB<sub>2</sub>-based therapeutics has been disappointing. It will be interesting to determine if CB<sub>2</sub> agonist efficacy in a specific preclinical model comes with a characteristic signaling “fingerprint”. If so, the development of CB<sub>2</sub> agonists only activating those signaling pathways may

result in efficacious drugs with fewer side effects. Functional selectivity has been demonstrated *in vivo* for 5HT<sub>2A</sub> as well as the opioid receptor ligands (Pradhan et al., 2011). It will be of great interest to see whether the functionally selective CB<sub>2</sub> ligands identified here will differ in their behavioral effects. Functional selectivity must also be considered when interpreting experiments examining CB<sub>2</sub> signaling. For example, WIN55,212-2 is often used as a ligand to test involvement of CB<sub>2</sub> in a particular pathway. If WIN55,212-2 does not activate this pathway well (e.g., VGCCs or receptor internalization) then false conclusions might be drawn on CB<sub>2</sub> involvement. Indeed, WIN55,212-2 may even antagonize the action of endogenous CB<sub>2</sub> ligands, such as 2-AG, further confounding interpretation. As Table 1 indicates, CB<sub>2</sub> ligands differ greatly in their activation of specific signaling pathways. This mandates caution in the interpretation of CB<sub>2</sub> signaling studies that employ only one cannabinoid as the ligand. More broadly, it encourages careful consideration of data utilizing a single ligand as pharmacological "proof" of the role (or not) of CB<sub>2</sub> in a physiological process. The pronounced functional selectivity of CB<sub>2</sub> ligands we have characterized in this study opens promising new avenues for drug discovery and for understanding the varied physiological roles of the CB<sub>2</sub> receptor.

## **Acknowledgements**

We would like to thank Douglas McHugh for help in optimizing the MAPK assay, Natasha Murataeva for help with data collection, Odile El Kouhen at Abbott Laboratories for assistance in obtaining A-836339 and comments on an earlier version of the manuscript, and Gerry Oxford for AtT20 cells and helpful discussions on their use. We would also like to thank Andrea Hohmann and Alex Makriyannis for the gift of AM1710, John Huffman for the gift of JWH018, Aron Lichtman for the gift of THCV, and Raphael Mechoulam for the gift of HU210.

**Authorship contributions:**

Participated in research design: Atwood, Mackie, Straiker.

Conducted experiments: Atwood, Haskins, Straiker, Wager-Miller.

Performed data analysis: Atwood, Straiker, Wager-Miller.

Wrote the manuscript: Atwood, Mackie, Straiker, Wager-Miller.

## References

- Anand P, Whiteside G, Fowler CJ and Hohmann AG (2009) Targeting CB2 receptors and the endocannabinoid system for the treatment of pain. *Brain Res Rev* **60**(1):255-266.
- Aramori I, Ferguson SS, Bieniasz PD, Zhang J, Cullen B and Cullen MG (1997) Molecular mechanism of desensitization of the chemokine receptor CCR-5: receptor signaling and internalization are dissociable from its role as an HIV-1 co-receptor. *EMBO J* **16**(15):4606-4616.
- Atwood BK, Huffman J, Straiker A and Mackie K (2010) JWH018, a common constituent of 'Spice' herbal blends, is a potent and efficacious cannabinoid CB(1) receptor agonist. *Br J Pharmacol.* **160**(3):585-593.
- Atwood BK, Lee D, Straiker A, Widlanski TS and Mackie K (2011) CP47,497-C8 and JWH073, commonly found in 'Spice' herbal blends, are potent and efficacious CB1 cannabinoid receptor agonists. *Eur J Pharmacol.* **659**(2-3):139-145.
- Atwood BK and Mackie K (2010) CB2: a cannabinoid receptor with an identity crisis. *Br J Pharmacol* **160**(3):467-479.
- Bayewitch M, Avidor-Reiss T, Levy R, Barg J, Mechoulam R and Vogel Z (1995) The peripheral cannabinoid receptor: adenylate cyclase inhibition and G protein coupling. *FEBS Lett* **375**(1-2):143-147.
- Benito C, Kim WK, Chavarría I, Hillard CJ, Mackie K, Tolón RM, Williams K, and



- Romero J (2005) A glial endogenous cannabinoid system is upregulated in the brains of macaques with simian immunodeficiency virus-induced encephalitis. *J Neurosci.* **25**(10):2530-6.
- Berdyshev EV (2000) Cannabinoid receptors and the regulation of immune response. *Chem Phys Lipids* **108**(1-2):169-190.
- Bingham B, Jones PG, Uveges AJ, Kotnis S, Lu P, Smith VA, Sun SC, Resnick L, Chlenov M, He Y, Strassle BW, Cummons TA, Piesla MJ, Harrison JE, Whiteside GT and Kennedy JD (2007) Species-specific in vitro pharmacological effects of the cannabinoid receptor 2 (CB2) selective ligand AM1241 and its resolved enantiomers. *Br J Pharmacol* **151**(7):1061-1070.
- Blankman JL, Simon GM and Cravatt BF (2007) A comprehensive profile of brain enzymes that hydrolyze the endocannabinoid 2-arachidonoylglycerol. *Chem Biol* **14**(12):1347-1356.
- Bolognini D, Costa B, Maione S, Comelli F, Marini P, Di Marzo V, Parolaro D, Ross RA, Gauson LA, Cascio MG and Pertwee RG The plant cannabinoid Delta9-tetrahydrocannabivarin can decrease signs of inflammation and inflammatory pain in mice. *Br J Pharmacol* **160**(3):677-687.
- Bouaboula M, Dussossoy D and Casellas P (1999) Regulation of peripheral cannabinoid receptor CB2 phosphorylation by the inverse agonist SR 144528. Implications for receptor biological responses. *J Biol Chem* **274**(29):20397-20405.
- Brown SM, Wager-Miller J and Mackie K (2002) Cloning and molecular characterization of the rat CB2 cannabinoid receptor. *Biochim Biophys Acta* **1576**(3):255-264.

Cabral GA and Griffin-Thomas L (2009) Emerging role of the cannabinoid receptor CB2 in immune regulation: therapeutic prospects for neuroinflammation. *Expert Rev Mol Med* **11**:e3.

Cravatt BF, Demarest K, Patricelli MP, Bracey MH, Giang DK, Martin BR and Lichtman AH (2001) Supersensitivity to anandamide and enhanced endogenous cannabinoid signaling in mice lacking fatty acid amide hydrolase. *Proc Natl Acad Sci U S A* **98**(16):9371-9376.

Daigle TL, Kearn CS and Mackie K (2008) Rapid CB1 cannabinoid receptor desensitization defines the time course of ERK1/2 MAP kinase signaling. *Neuropharmacology* **54**(1):36-44.

Felder CC, Joyce KE, Briley EM, Mansouri J, Mackie K, Blond O, Lai Y, Ma AL and Mitchell RL (1995) Comparison of the pharmacology and signal transduction of the human cannabinoid CB1 and CB2 receptors. *Mol Pharmacol* **48**(3):443-450.

Finn AK and Whistler JL (2001) Endocytosis of the mu opioid receptor reduces tolerance and a cellular hallmark of opiate withdrawal. *Neuron* **32**(5):829-839.

Gallant M, Dufresne C, Gareau Y, Guay D, Leblanc Y, Prasit P, Rochette C, Sawyer N, Slipetz DM, Tremblay N, Metters KM, and Labelle M (1996) New class of potent ligands for the human peripheral cannabinoid receptor. *Bioorg Med Chem Lett* **6**(19): 2263–2268.

Griffin G, Tao Q and Abood ME (2000) Cloning and pharmacological characterization of the rat CB(2) cannabinoid receptor. *J Pharmacol Exp Ther* **292**(3):886-894.

Grimsey NL, Goodfellow CE, Dargunow M, and Glass M (2011)

- Cannabinoid receptor 2 undergoes Rab5-mediated internalization and recycles via a Rab11-dependent pathway. *Biochim Biophys Acta* **1813**(8):1554-1560.
- Howlett AC, Barth F, Bonner TI, Cabral G, Casellas P, Devane WA, Felder CC, Herkenham M, Mackie K, Martin BR, Mechoulam R and Pertwee RG (2002) International Union of Pharmacology. XXVII. Classification of cannabinoid receptors. *Pharmacol Rev* **54**(2):161-202.
- Hsieh C, Brown S, Derleth C and Mackie K (1999) Internalization and recycling of the CB1 cannabinoid receptor. *J Neurochem* **73**(2):493-501.
- Huestis MA, Gorelick DA, Heishman SJ, Preston KL, Nelson RA, Moolchan ET and Frank RA (2001) Blockade of effects of smoked marijuana by the CB1-selective cannabinoid receptor antagonist SR141716. *Arch Gen Psychiatry* **58**(4):322-328.
- Huffman JW, Dong D, Martin BR and Compton DR (1994) Design, Synthesis and Pharmacology of Cannabimimetic Indoles. *Bioorganic & Medicinal Chemistry Letters* **4**(4):563-566.
- Ibrahim MM, Deng H, Zvonok A, Cockayne DA, Kwan J, Mata HP, Vanderah TW, Lai J, Porreca F, Makriyannis A, Malan TP Jr. (2003) Activation of CB2 cannabinoid receptors by AM1241 inhibits experimental neuropathic pain: pain inhibition by receptors not present in the CNS. *Proc Natl Acad Sci U S A*. **100**(18):10529-33.
- Kearn CS, Blake-Palmer K, Daniel E, Mackie K and Glass M (2005) Concurrent stimulation of cannabinoid CB1 and dopamine D2 receptors enhances heterodimer formation: a mechanism for receptor cross-talk? *Mol Pharmacol* **67**(5):1697-1704.

- Khanolkar AD, Lu D, Ibrahim M, Duclos RI Jr, Thakur GA, Malan TP Jr, Porreca F, Veerappan V, Tian X, George C, Parrish DA, Papahatjis DP, Makriyannis A. (2007) Cannabilactones: a novel class of CB2 selective agonists with peripheral analgesic activity. *J Med Chem.* **50**(26):6493-500.
- Koch T and Holtt V (2008) Role of receptor internalization in opioid tolerance and dependence. *Pharmacol Ther* **117**(2):199-206.
- Koch T, Widera A, Bartsch K, Schulz S, Brandenburg LO, Wundrack N, Beyer A, Grecksch G and Holtt V (2005) Receptor endocytosis counteracts the development of opioid tolerance. *Mol Pharmacol* **67**(1):280-287.
- Lauckner JE, Jensen JB, Chen HY, Lu HC, Hille B and Mackie K (2008) GPR55 is a cannabinoid receptor that increases intracellular calcium and inhibits M current. *Proc Natl Acad Sci U S A* **105**(7):2699-2704.
- Ligresti A, Cascio MG and Di Marzo V (2005) Endocannabinoid metabolic pathways and enzymes. *Curr Drug Targets CNS Neurol Disord* **4**(6):615-623.
- Long JZ, Li W, Booker L, Burston JJ, Kinsey SG, Schlosburg JE, Pavon FJ, Serrano AM, Selley DE, Parsons LH, Lichtman AH and Cravatt BF (2009) Selective blockade of 2-arachidonoylglycerol hydrolysis produces cannabinoid behavioral effects. *Nat Chem Biol* **5**(1):37-44.
- Mackie K (2005) Distribution of cannabinoid receptors in the central and peripheral nervous system. *Handb Exp Pharmacol*(168):299-325.
- Miller A and Stella N (2008) CB2 receptor-mediated migration of immune cells: it can go either way. *Br J Pharmacol.* **153**(2):299-308.

- Monory K, Blaudzun H, Massa F, Kaiser N, Lemberger T, Schutz G, Wotjak CT, Lutz B and Marsicano G (2007) Genetic dissection of behavioural and autonomic effects of Delta(9)-tetrahydrocannabinol in mice. *PLoS Biol* **5**(10):e269.
- Mukherjee S, Adams M, Whiteaker K, Daza A, Kage K, Cassar S, Meyer M and Yao BB (2004) Species comparison and pharmacological characterization of rat and human CB2 cannabinoid receptors. *Eur J Pharmacol* **505**(1-3):1-9.
- Pradhan AA, Befort K, Nozaki C, Gavériaux-Ruff C, Kieffer BL. (2011) The delta opioid receptor: an evolving target for the treatment of brain disorders. *Trends Pharmacol Sci.* **32**(10):581-590.
- Rahn EJ, Thakur GA, Wood JA, Zvonok AM, Makriyannis A, Hohmann AG. (2011) Pharmacological characterization of AM1710, a putative cannabinoid CB2 agonist from the cannabiolactone class: antinociception without central nervous system side-effects. *Pharmacol Biochem Behav.* **98**(4):493-502.
- Rajagopal S, Rajagopal K and Lefkowitz RJ (2010) Teaching old receptors new tricks: biasing seven-transmembrane receptors. *Nat Rev Drug Discov* **9**(5):373-386.
- Ross RA, Coutts AA, McFarlane SM, Anavi-Goffer S, Irving AJ, Pertwee RG, MacEwan DJ and Scott RH (2001) Actions of cannabinoid receptor ligands on rat cultured sensory neurones: implications for antinociception. *Neuropharmacology* **40**(2):221-232.
- Schuehly W, Paredes JM, Kleyer J, Huefner A, Anavi-Goffer S, Raduner S, Altmann KH, and Gertsch J (2011) Mechanisms of Osteoclastogenesis Inhibition by a Novel Class of Biphenyl-Type Cannabinoid CB(2) Receptor Inverse Agonists. *Chem Biol* **18**(8):1053-1064.

- Shoemaker JL, Ruckle MB, Mayeux PR and Prather PL (2005) Agonist-directed trafficking of response by endocannabinoids acting at CB2 receptors. *J Pharmacol Exp Ther* **315**(2):828-838.
- Tao Q and Abood M (1998) Mutation of a Highly Conserved Aspartate Residue in the Second Transmembrane Domain of the Cannabinoid Receptors, CB1 and CB2, Disrupts G-Protein Coupling. *J Pharmacol Exp Ther* **285**(2):651-658.
- Thomas A, Stevenson LA, Wease KN, Price MR, Baillie G, Ross RA, and Pertwee RG. (2005) Evidence that the plant cannabinoid Delta9-tetrahydrocannabivarin is a cannabinoid CB1 and CB2 receptor antagonist. *Br J Pharmacol.* **146**(7):917-26.
- Urban JD, Clarke WP, von Zastrow M, Nichols DE, Kobilka B, Weinstein H, Javitch JA, Roth BL, Christopoulos A, Sexton PM, Miller KJ, Spedding M and Mailman RB (2007) Functional selectivity and classical concepts of quantitative pharmacology. *J Pharmacol Exp Ther* **320**(1):1-13.
- von Zastrow M, Svingos A, Haberstock-Debic H and Evans C (2003) Regulated endocytosis of opioid receptors: cellular mechanisms and proposed roles in physiological adaptation to opiate drugs. *Curr Opin Neurobiol* **13**(3):348-353.
- Whistler JL, Chuang HH, Chu P, Jan LY and von Zastrow M (1999) Functional dissociation of mu opioid receptor signaling and endocytosis: implications for the biology of opiate tolerance and addiction. *Neuron* **23**(4):737-746.

- Wotherspoon G, Fox A, McIntyre P, Colley S, Bevan S and Winter J (2005) Peripheral nerve injury induces cannabinoid receptor 2 protein expression in rat sensory neurons. *Neuroscience* **135**(1):235-245.
- Wu DF, Yang LQ, Goschke A, Stumm R, Brandenburg LO, Liang YJ, Holtt V and Koch T (2008) Role of receptor internalization in the agonist-induced desensitization of cannabinoid type 1 receptors. *J Neurochem* **104**(4):1132-1143.
- Xi ZX, Peng XQ, Li X, Song R, Zhang HY, Liu QR, Yang HJ, Bi GH, Li J, Gardner EL. Brain cannabinoid CB(2) receptors modulate cocaine's actions in mice. *Nat Neurosci.* **14**(9):1160-6.
- Yao BB, Hsieh G, Daza AV, Fan Y, Grayson GK, Garrison TR, El Kouhen O, Hooker BA, Pai M, Wensink EJ, Salyers AK, Chandran P, Zhu CZ, Zhong C, Ryther K, Gallagher ME, Chin CL, Tovcimak AE, Hradil VP, Fox GB, Dart MJ, Honore P and Meyer MD (2009) Characterization of a cannabinoid CB2 receptor-selective agonist, A-836339 [2,2,3,3-tetramethyl-cyclopropanecarboxylic acid [3-(2-methoxy-ethyl)-4,5-dimethyl-3H-thiazol-(2Z)-ylidene]-amide], using in vitro pharmacological assays, in vivo pain models, and pharmacological magnetic resonance imaging. *J Pharmacol Exp Ther* **328**(1):141-151.
- Yiangou Y, Facer P, Durrenberger P, Chessell IP, Naylor A, Bountra C, Banati RR and Anand P (2006) COX-2, CB2 and P2X7-immunoreactivities are increased in activated microglial cells/macrophages of multiple sclerosis and amyotrophic lateral sclerosis spinal cord. *BMC Neurol* **6**:12.

Zhang J, Hoffert C, Vu HK, Groblewski T, Ahmad S and O'Donnell D (2003) Induction of CB2 receptor expression in the rat spinal cord of neuropathic but not inflammatory chronic pain models. *Eur J Neurosci* **17**(12):2750-2754.



**Footnote:**

This work was supported by the National Institutes of Health -- National Institute on Drug Abuse [Grants DA011322, DA021696, DA009158] and the National Institutes of Health – National Institute for Research Resources [Grant RR025761]

## Legends for Figures

### Figure 1

#### **CP55,940 and WIN55,212-2 differ in their abilities to internalize rCB<sub>2</sub> but not rCB<sub>1</sub> cannabinoid receptors**

(A) In rCB<sub>1</sub> and rCB<sub>2</sub> expressing HEK293 cells 100nM CP55,940 results in receptor internalization (n=6-26 for each time point). (B) 2 hours of exposure to CP55,940 internalized rCB<sub>1</sub> and rCB<sub>2</sub> in a concentration-dependent manner (n=3-26 for each concentration). (C) 1 μM rimonabant and 1 μM AM630 prevent receptor internalization by 100 nM CP55,940 treatment in rCB<sub>1</sub> (n=3) and rCB<sub>2</sub> cells (n=10), respectively. (D) 100nM WIN55,212-2 results in robust rCB<sub>1</sub>, but not rCB<sub>2</sub> receptor internalization (n=7-11). (E) 2 hours of exposure to WIN55,212-2 internalized rCB<sub>1</sub> in a concentration-dependent manner, but not rCB<sub>2</sub> (n=4-6). (F) 1 μM rimonabant prevents receptor internalization by 100 nM WIN55,212-2 treatment in rCB<sub>1</sub> (n=5) but AM630 does not alter the effect of WIN55,212-2 on rCB<sub>2</sub> cells (n=4). (G) Representative images of rCB<sub>1</sub> and rCB<sub>2</sub> cells treated with 100 nM CP55,940 or 100 nM WIN55,212-2 for 2 hours. Co-treatment with 1 μM rimonabant and 1 μM AM630 are also shown. Scale bars = 20 μm. Data in (A) through (F) analyzed using unpaired Student's t-tests. \*: p<0.05, \*\*: p<0.01, \*\*\*: p<0.001.

### Figure 2

#### **Concentration response curves for internalization by various agonists and ligands in rCB<sub>1</sub>- and rCB<sub>2</sub>-expressing HEK293 cells**

Concentration response curves for rCB<sub>1</sub> (A-C: left) and rCB<sub>2</sub> (A-C: right) expressing HEK293 cells following 2 hours of treatments with: (A) aminoalkylindoles (n=3-5), (B) classical cannabinoids (n=3-6), and (C) endocannabinoids (n=3-5). (D) the iminothiazole A-836339 (n=3-5) and the cannabillactone AM1710 (n=4). CP47,497-C8 data from Atwood et al., 2011 included for comparison. (E) Concentration response curves for rCB<sub>2</sub> cells treated with the CB<sub>2</sub> antagonists SR14428 and AM630 (n=4-5).

### Figure 3

#### **WIN55,212-2 and other aminoalkylindoles antagonize CP55,940-induced rCB<sub>2</sub> internalization**

(A) Time course of 100 nM CP55,940-induced internalization of rCB<sub>2</sub> in HEK293 cells. Co-treatment with 100 nM and 1  $\mu$ M WIN55,212-2 attenuates CP55,940 mediated internalization. \*: vs. CP55,940 alone.  $\square$ †: 100 nM vs. 1  $\mu$ M WIN55,212-2 (n=4-6). (B) WIN55,212-2 does not have an effect on CP55,940 mediated rCB<sub>1</sub> internalization (n=3-12). (C) Representative images of rCB<sub>1</sub> and rCB<sub>2</sub> HEK293 cells treated with the combination of 100 nM CP55,940 and 1  $\mu$ M WIN55,212-2. Scale bars = 20  $\mu$ m. (D) rCB<sub>1</sub> or rCB<sub>2</sub> cells were co-treated with 100 nM CP55,940 and increasing concentrations of WIN55,212-2 (closed symbols) or alternatively co-treated with 100 nM WIN55,212-2 and increasing concentrations of CP55,940 (open symbols). \*: CP + WIN vs. WIN + CP (n=3-15). (E) Individual concentration curves of CP55,940 with indicated concentrations of WIN55,212-2 co-treatments (n=6-27). (F) Schild plot constructed from data in (E). The slope indicates that the interaction between CP55,940 and WIN55,212-2 is competitive. (G) Co-treatments of rCB<sub>2</sub> HEK293 cells with 10 nM CP55,940 and 100 nM or 1  $\mu$ M of the indicated ligands (n=3-17). \*: vs. CP55,940 alone. Data in (A), (B),

and (G) analyzed using one-way ANOVA with Bonferroni's multiple comparison test.

Data in (D) analyzed using Student's t-test. \*:  $p < 0.05$ , \*\*/††:  $p < 0.01$ , \*\*\*/†††:  $p < 0.001$ .

#### Figure 4

##### **CP55,940 and WIN55,212-2 promote MAPK activation in rCB<sub>1</sub> and rCB<sub>2</sub> expressing HEK293 cells**

(A) Time course of MAPK activation in rCB<sub>1</sub> HEK293 cells with 100 nM of CP55,940 and 100 nM WIN55,212-2 (n=9-21). (B) Same as in (A), but with rCB<sub>2</sub> HEK293 cells (n=7-22). (C) Concentration-response curves for 5 minute treatments with increasing concentrations of CP55,940 and WIN55,212-2 in rCB<sub>1</sub> HEK293 cells. 1  $\mu$ M rimonabant blocks MAPK activation by 100 nM of either agonist (n=4-21). (D) Concentration-response curves for 5 minute treatments with increasing concentrations of CP55,940 or WIN55,212-2 in rCB<sub>2</sub> HEK293 cells (n=5-22). 1  $\mu$ M AM630 blocks MAPK activation by 100 nM of either agonist. Data analyzed using unpaired Student's t-test. \*: CP55,940 vs. WIN55,212-2. †: CP55,940 or WIN55,212-2 vs. antagonist. \*:  $p < 0.05$ , \*\*:  $p < 0.01$ , \*\*\*/†††:  $p < 0.001$ .

#### Figure 5

##### **CP55,940 and WIN55,212-2 promote recruitment of $\beta$ -arrestin<sub>2</sub> to the membrane in rCB<sub>1</sub> and rCB<sub>2</sub> expressing HEK293 cells**

(A) HEK293 cells transiently expressing rCB<sub>1</sub> and  $\beta$ -arrestin<sub>2</sub>-mRFP were treated with 100 nM CP55,940 or 100 nM WIN55,212-2 with or without 1  $\mu$ M rimonabant. Top panels show  $\beta$ -arrestin<sub>2</sub>-mRFP. Bottom panels show staining for rCB<sub>1</sub> (anti-HA primary

antibody). Arrowheads indicate examples of membrane recruitment of  $\beta$ -arrestin<sub>2</sub>. Scale bars = 10  $\mu$ m. (B) Same as in (A) but with rCB<sub>2</sub> transiently expressed instead of rCB<sub>1</sub>. 100 nM CP55,940, 1  $\mu$ M WIN55,212-2 and 1  $\mu$ M AM630 were used in the treatments. (C) Quantification of data from rCB<sub>1</sub> cells (n=6-14), rCB<sub>2</sub> cells (n=10-13), and native HEK293 cells (n=5). Increases in membrane/cytosol ratio indicate  $\beta$ -arrestin<sub>2</sub> membrane recruitment. Data in (C) and (D) analyzed using one-way ANOVA with Bonferroni's multiple comparison test. \*: vs. untreated. □†: CP55,940 or WIN55,212-2 vs. antagonist. \*: p<0.05, ††: p<0.01, \*\*\*/†††: p<0.001.

## Figure 6

### **CP55,940, but not WIN55,212-2, activates mCB<sub>2</sub> to inhibit voltage gated calcium channels.**

Barium currents in AtT20 cells were elicited by depolarizing the cells to 0 mV for 30 ms from a holding potential of -70 mV. In mCB<sub>2</sub> expressing AtT20 cells, 100 nM WIN55,212-2 (A) had no effect on the amplitude of recorded currents, whereas 100 nM CP55,940 (B) inhibited calcium channels. (C) 1  $\mu$ M AM630 increased the magnitude of barium currents. (D) CP55,940 inhibited voltage gated calcium channels in a concentration dependent manner (n=4-17), whereas 100 nM (n=6) and 1  $\mu$ M WIN55,212-2 did not (n=7). \*: vs. CP55,940. (E) 1  $\mu$ M AM630 blocked the effects of 100 nM CP55,940 in mCB<sub>2</sub> expressing AtT20 cells (n=4) and increased the magnitude of barium currents on its own (as seen by a negative inhibition) (n=15). 100 nM CP55,940 had no effect on calcium channels in wild type untransfected cells (n=5), but was able to inhibit calcium channels in rCB<sub>1</sub> expressing AtT20 cells (n=6). 100 nM WIN55,212-2 inhibited voltage gated calcium channels in rCB<sub>1</sub> expressing AtT20 cells

(n=6). 10  $\mu$ M oxotremorine-M (oxo-M) inhibited calcium channels in untransfected HEK cells (n=9). This inhibition was decreased in AtT20 cells stably expressing mCB<sub>2</sub> (n=9). \*: vs. CP55,940 treatment of mCB<sub>2</sub> AtT20 cells. #: vs. WIN55,212-2 treatment of mCB<sub>2</sub> AtT20 cells. †: vs Oxo-M treatment of mCB<sub>2</sub> AtT20 cells. (F) 1  $\mu$ M WIN55,212-2 does not affect the inhibition of VGCCs by 100 nM CP55,940. Data in (D) and (F) were analyzed using unpaired Student's t-test. Data in (E) were analyzed using one-way ANOVA with Bonferroni's multiple comparison test. \*/†/#: p<0.05, \*\*\*: p<0.001.

**Table 1**

Drug <sup>a,b</sup>	Internalization (% Basal Surface Levels)	MAPK Activation (% Basal) <sup>c</sup>	$\beta$ -arrestin recruitment Membrane/Cytosol Ratio <sup>d</sup>	VGCC Inhibition % Inhibition <sup>c</sup>	CB <sub>2</sub> K <sub>i</sub> (nM)
CP55,940	61 ± 1.9	130 ± 3.6***	1.9 ± 0.11***	17 ± 2.4**	0.64-2.8 <sup>e</sup>
WIN55,212-2	100 ± 3.2	130 ± 4.9**	1.1 ± 0.035 ns	-3.4 ± 3.2 ns	0.28-16.2 <sup>e</sup>
AM1241	100 ± 6.6	100 ± 3.5 ns	1.0 ± 0.056 ns	-0.83 ± 1.1 ns	3.4 <sup>i</sup>
JWH015	91 ± 5.8	120 ± 2.4***	1.1 ± 0.030 ns	-3.9 ± 2.1 *	14-430 <sup>e</sup>
JWH133	77 ± 3.3	120 ± 2.7***	1.2 ± 0.058***	18 ± 6.2 *	3.4 <sup>e</sup>
THC	100 ± 2.0	120 ± 2.2***	1.1 ± 0.058 ns	-7.0 ± 2.7 ns	1.7-75 <sup>e</sup>
THCV	88 ± 2.0	120 ± 2.1**	1.0 ± 0.032 ns	-17 ± 7.4 ns	63-75 <sup>g</sup>
AM1710	71 ± 3.0	120 ± 3.2**	1.3 ± 0.060***	-3.1 ± 4.1 ns	6.7 <sup>h</sup>
A-836339	82 ± 2.1	120 ± 2.5***	1.2 ± 0.039**	16 ± 4.1 ns	0.64 <sup>i</sup>
2-AG	81 ± 6.3	130 ± 8.1*	1.1 ± 0.025 ns	33 ± 6.2*	140-1400 <sup>e</sup>
GW405833	no data	no data	no data	-2.5 ± 1.4	12 <sup>j</sup>
AM630	100 ± 2.1	97 ± 1.3 ns	1.0 ± 0.022 ns	-12 ± 2.4**	31 <sup>e</sup>
SR144528	130 ± 4.5	99 ± 2.0 ns	0.93 ± 0.039 ns	-10 ± 3.2*	0.040-15 <sup>e</sup>

<sup>a</sup> 10  $\mu$ M 2-AG was used for internalization, 5  $\mu$ M 2-AG for MAPK,  $\beta$ -arrestin and VGCC experiments. 1  $\mu$ M for all other drugs

<sup>b</sup> internalization (n=12), MAPK activation (n=6-15),  $\beta$ -arrestin recruitment (n=5-15), VGCC Inhibition (n=4-17)

<sup>c</sup> \*: vs. untransfected control cells. \*: p<0.05, \*\*: p<0.01, \*\*\*: p<0.001, ns: not significant, GW405833 not tested in control cells

<sup>d</sup> \*:vs. untreated control. \*: p<0.05, \*\*: p<0.01, \*\*\*: p<0.001, ns: not significant

<sup>e</sup> as reviewed in Miller and Stella, 2008, <sup>f</sup>Ibrahim et al., 2003, <sup>g</sup>Thomas et al., 2005, <sup>h</sup>Khanolkar et al., 2007, <sup>i</sup>Yao et al., 2008, <sup>j</sup>Gallant et al., 1996

## Evidence for functionally selective CB<sub>2</sub> ligands

Cannabinoid ligands from multiple classes were tested for their abilities to activate ERK1/2 MAPK in rCB<sub>2</sub> expressing HEK293 cells, promote  $\beta$ -arrestin<sub>2</sub> membrane recruitment in HEK293 cells transiently transfected with rCB<sub>2</sub> and  $\beta$ -arrestin<sub>2</sub>-mRFP, and inhibit VGCCs in mCB<sub>2</sub> expressing AtT20. Positive values reflect inhibition of VGCCs and negative values reflect activation (e.g., inverse agonism). Protocols for each experiment were identical to those done in Figs. 4, 5 and 6. Data for ERK1/2 and VGCC experiments were analyzed using unpaired Student's t-test vs. native HEK293 or

native AtT20 cells, respectively. Data for  $\beta$ -arrestin were analyzed using one-way ANOVA with Dunnett post-tests. Data for internalization from Figs. 1 and 2 and binding data obtained from the cited references are included for additional comparison.



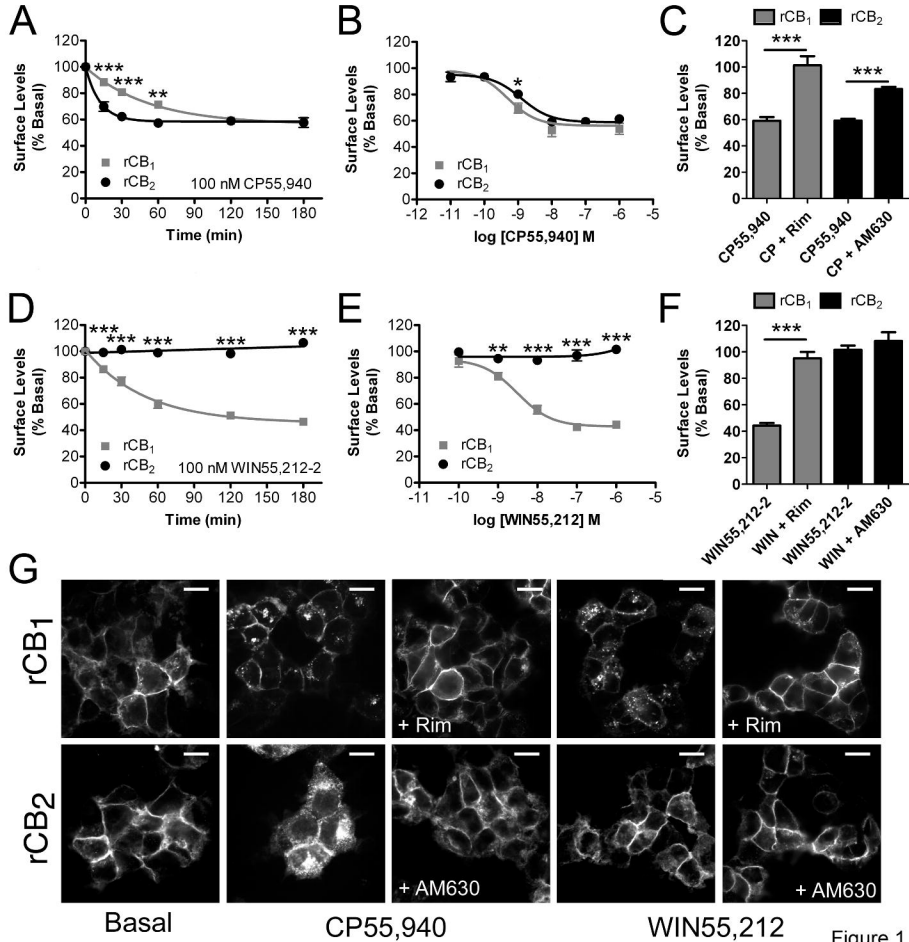


Figure 1

Figure 2

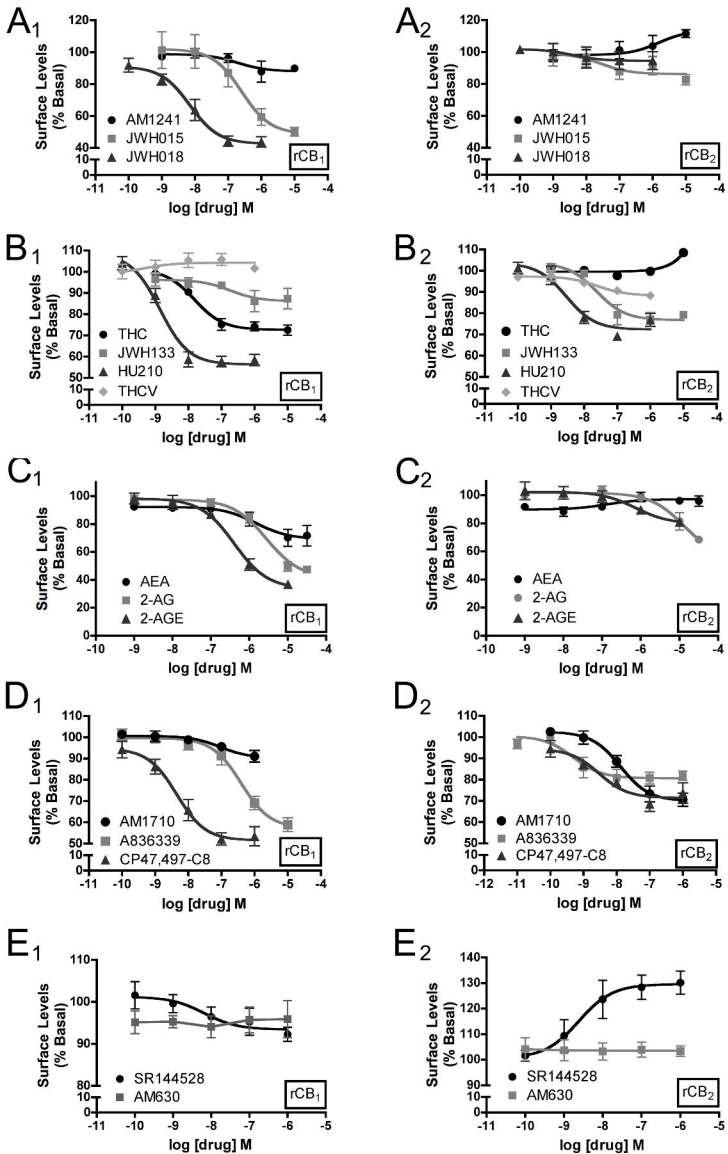
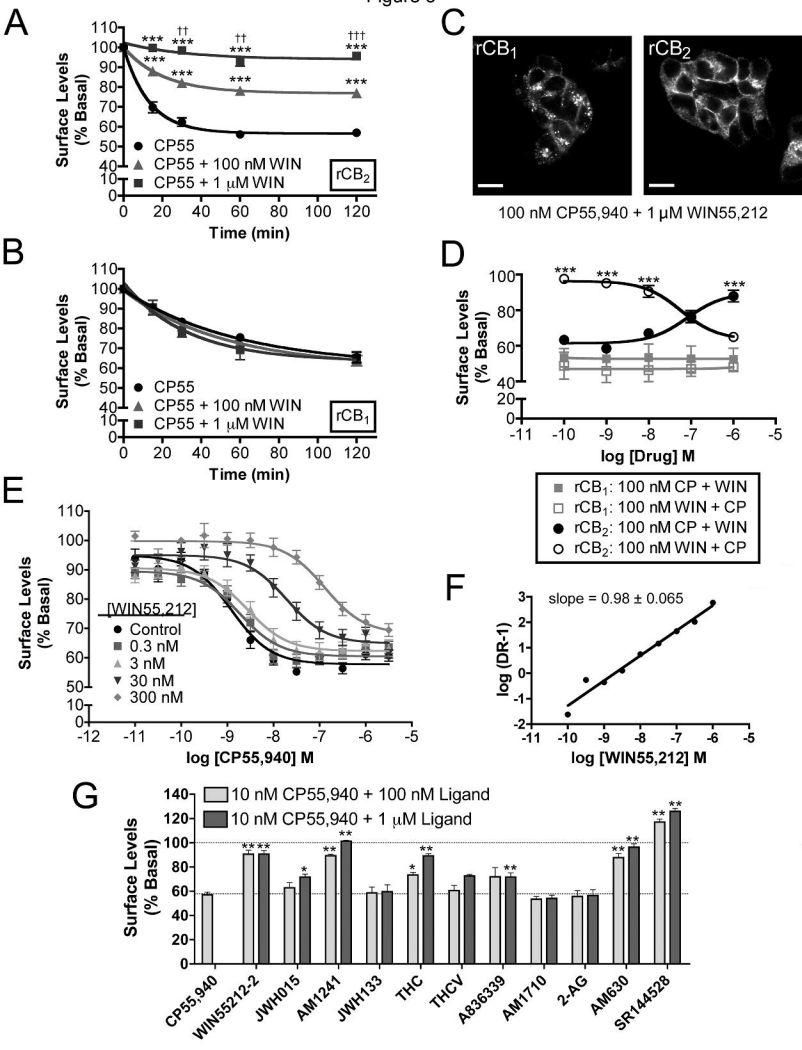


Figure 3



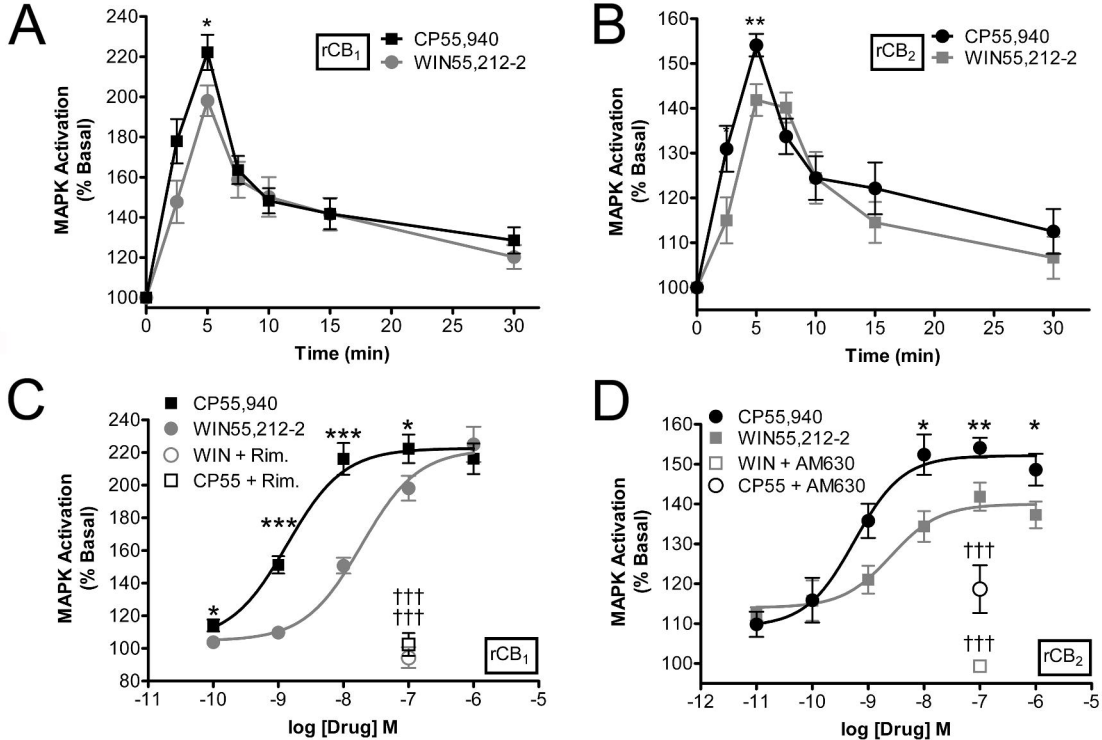
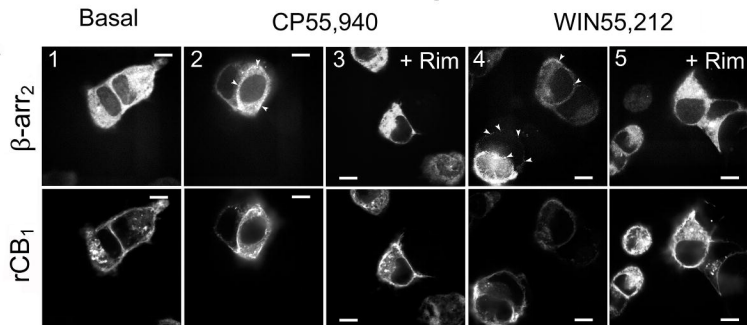
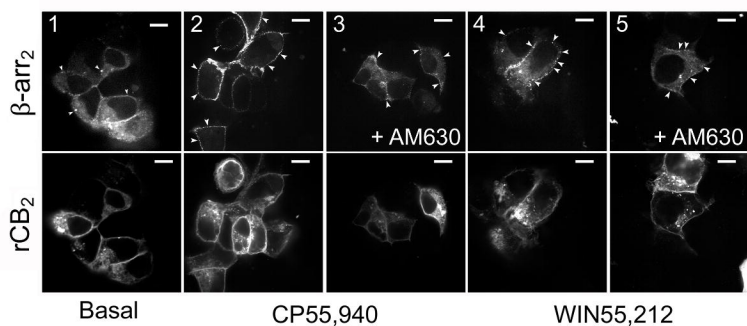
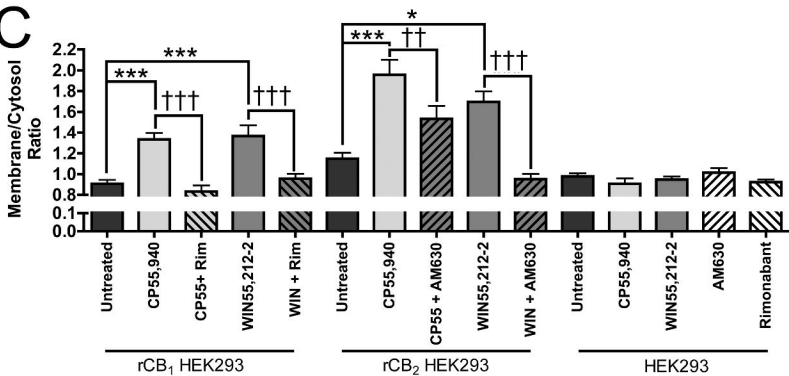


Figure 4

**A****B****C**

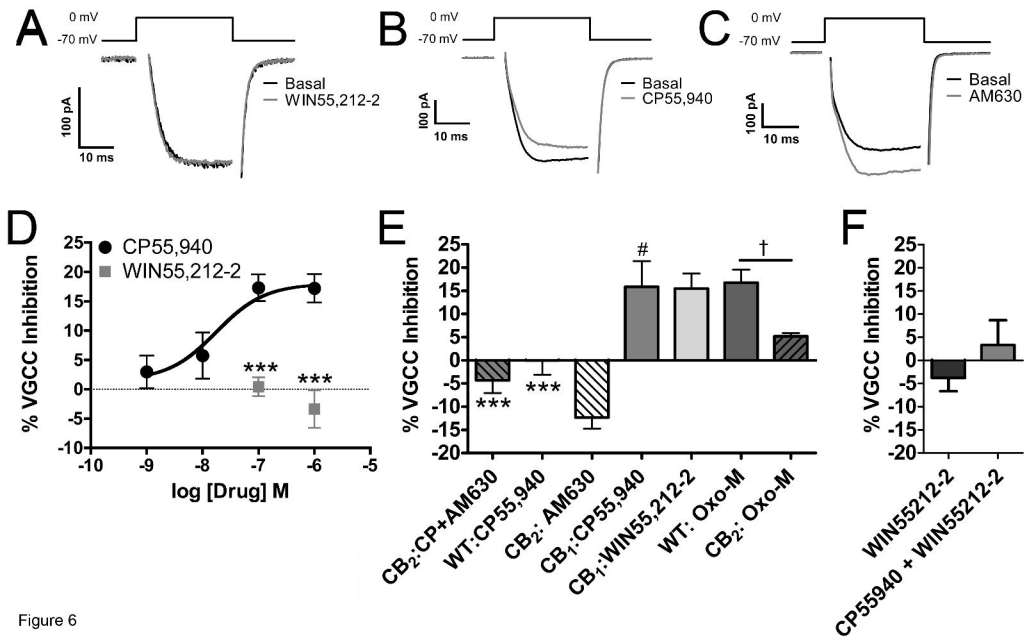


Figure 6